



INTERNATIONAL ATOMIC ENERGY AGENCY
UNITED NATIONS EDUCATIONAL, SCIENTIFIC AND CULTURAL ORGANIZATION



INTERNATIONAL CENTRE FOR THEORETICAL PHYSICS
34100 TRIESTE (ITALY) - P.O.B. 586 - MIRAMARE - STRADA COSTIERA 11 - TELEPHONE: 2240-1
CABLE: CENTRATOM - TELEX 460892 - I

SMR/291 - 25

SPRING COLLEGE IN CONDENSED MATTER
ON
"THE INTERACTION OF ATOMS & MOLECULES WITH SOLID SURFACES"
(25 April - 17 June 1988)

ELECTRONIC THEORY OF CHEMISORPTION

D. SPANJAARD
Laboratoire de Physique des Solides
Bat. 510
Université Paris-Sud
F-91405 Orsay Cédex
France

and

M.C. DESJONQUERES
IRF/DPhG/PAS
Centre d'Etudes Nucléaires de Saclay
F-91191 Gif-sur-Yvette
France

These are preliminary lecture notes, intended only for distribution to participants.

ELECTRONIC THEORY OF CHEMISORPTION

D. Spanjaard⁽¹⁾ and M. C. Desjonquères⁽²⁾⁽¹⁾ Laboratoire de Physique des Solides, Bât. 510, Université Paris-Sud,
F91405 Orsay Cédex France⁽²⁾ IRF/DPHG/PAS, Centre d'Etudes Nucléaires de Saclay -
F91191 Gif-sur-Yvette Cédex, France

1 - INTRODUCTION

In surface physics, one calls adsorption the accumulation at the solid-vapour interface of atoms or molecules coming from the gas phase. One usually classifies adsorption phenomena into two domains according to the energy E_B involved in the bonding :

- when $|E_B| \lesssim 0.5$ eV, the adsorbate is said to be physisorbed on the surface. In physisorption, the adsorbate binds to the substrate via Van der Waals forces which are due to dipole-dipole interactions. A typical example is the rare-gas adsorption.

- when $|E_B| \gtrsim 0.5$ eV, the adsorbate is said to be chemisorbed. The bond between the adsorbate and the substrate is of chemical type i. e. it involves sharing (covalent bond) or transfer (ionic bond) of electrons. This is the case for O, N, H... on transition metals. This domain is obviously the most important in view of its practical applications (catalysis, corrosion...) and we will limit ourselves to this phenomenon.

The adsorption theory can be tackled using three complementary approaches :

- the macroscopic or thermodynamical approach which gives useful relationships between measurable quantities of the system : for instance, the relation between the amount of adsorbates and the pressure.
- the microscopic approach which aims at calculating the interaction between the adsorbate and the substrate within the quantum theory.
- the statistical methods which link the above approaches by relating macroscopic and microscopic physical quantities.

In these lectures, we will limit ourselves to the microscopic approach. Within this approach a complete knowledge of chemisorption phenomena requires the determination of

- the geometrical structure of the system (adsorption site, bond length...)
- the adsorbate binding and diffusion activation energies
- the charge transfer
- the electronic structure of the adsorbate and substrate
- the vibration frequencies.

These physical quantities can be measured more or less directly by a variety of experimental techniques. Let us mention for example ⁽¹⁾ :

- field ion microscopy (FIM), low energy electron diffraction (LEED), surface extended X-ray absorption fine structure (SEXAFS), surface core level spectroscopy (i. e. electron spectroscopy for chemical analysis-ESCA-at the surface) for the geometrical structure,
- microcalorimetry, thermal desorption, FIM for binding and diffusion energies,
- work function measurement, surface core level spectroscopy for charge transfers,

- UV and X-ray photoemission (UPS, XPS), field emission microscopy (FEM), ion neutralisation spectroscopy (INS)... for the electronic structure,
- electron energy loss spectroscopy (EELS), neutron diffraction, Raman spectroscopy... for the vibration frequencies.

Although these experimental data are sometimes rather spread for a given system, they undoubtedly exhibit systematic trends which we will now summarize :

- the bond-length (i. e. the distance between the adsorbate and its nearest neighbours) increases with the coordination number Z of the adsorbate as shown in Table I for O, S, Se on Ni (111) and (100)⁽²⁾. Other examples can be found in ref. ⁽³⁾. The same trend is also obeyed by surface atoms which, due to their broken bonds, come closer to the subsurface plane i. e. there is a contraction of the first interlayer spacing ⁽⁴⁾ which decreases or even vanishes in the presence of adsorbed atoms. Similarly one observes a dilatation of the interatomic spacing a for transition metals exhibiting a phase transition from a body centered cubic structure (8 nearest neighbours) to a compact structure (12 nearest neighbours) : for instance $a = 2.48 \text{ \AA}$ for bcc Fe and 2.52 \AA for fcc Fe,
- the most stable adsorption position is usually the site with the largest coordination number available on the surface ⁽⁵⁾. Let us notice however that some chemisorbed atoms do not occupy the site with maximum coordination : it is known that, on the (100) face of W, H sits at the bridge rather than at a centered position ⁽⁶⁾,
- the variation of binding energy with the crystallographic orientation of the surface plane (anisotropy) is always smaller than expected from simple arguments such as the number of bonds even though there is a large straggling in experimental data ⁽⁶⁾,
- the variation of the binding energy has been studied either for a series of

adsorbates on a given substrate or for a given adsorbate on a series of substrates. Fig. 1 shows the results obtained for 5d adatoms on W (111), (112) and Ir (111) ⁽⁷⁾ which follow a parabolic behaviour similar to that of the cohesive energies. In Fig. 2 we give the variation of the binding energies of N, O, F, H ⁽⁸⁾⁽⁹⁾ along a transition series which decreases continuously when the substrate d band fills,

- the surface diffusion activation energies have only been measured for 5d adatoms on various faces of W ⁽⁹⁾. They exhibit a maximum near the middle of the series similarly to their binding energy (Fig. 3). More qualitatively it is known that transition adatoms deposited on the pole of a FIM tip are most often reflected by the edge of the tip ⁽¹⁰⁾. One also observes that the diffusion of adatoms along a smooth ledge step is little perturbed by the presence of the step ⁽¹¹⁾,
- finally the ability of transition metal surfaces to dissociate simple molecules (N_2 , O_2 , NO ...) decreases along a transition series (see Table II ⁽¹²⁾).

One needs therefore a theory which can rationalise all these results and make good predictions for not yet investigated systems. This is actually a very difficult task since, ideally, one should determine the geometrical and electronic structures self-consistently by minimizing the total energy of the system. Two main tracks have been followed based either on the quantum chemistry methods or on solid state physics techniques. However none of these lines of attack are fully appropriate since the former most often deals with a finite number of atoms while the latter usually treats systems with three dimensional periodicity. We will develop here mainly the methods derived from solid state physics and we will show how these methods can be modified to deal with non-periodic systems. We will also give a brief outline of the most usual quantum chemistry methods. Finally we will only consider the adsorption on

metals of isolated atoms or molecules i. e. we will assume that the adsorbate coverage is so small that the interaction between adsorbates can be neglected.

2 - OUTLINE OF THE PROBLEM

Let us consider an atom X approaching the surface of a metal the Fermi level and the work function of the latter being respectively E_F and ϕ . Let us call I and A respectively the ionization and affinity energies of the free atom (i. e. at an infinite distance from the surface). From these quantities, one usually defines an effective Coulomb integral U which is the energy involved in the reaction :



i. e.

$$U = I - A \quad (2)$$

(U is positive since $A < I$).

When the atom is far from the metal surface, the main interaction comes from classical electric image effects and leads to a shift of ionization and affinity levels (Fig. 4) which can be easily calculated⁽¹²⁾ :

2 - 1. Ionization level

The image force acting on the outgoing electron is (Fig. 5) :

$$F = -\frac{e^2}{4z^2} + \frac{e^2}{(d+z)^2} \quad (3)$$

The first and second terms are respectively due to its own image and to the ion image. z being large, the resulting force is repulsive and therefore the ionization energy is decreased by an amount which is given by :

$$W = \int_d^\infty F dz = \frac{e^2}{4d} = V_{Im} \quad (4)$$

and therefore the effective ionization energy is :

$$I_{eff} = I - \frac{e^2}{4d} = I - V_{Im} \quad (5)$$

2 - 2. Affinity level

Similarly when approaching an additional electron towards the adsorbate, only its image contributes to the image force. This force is attractive and the modification of the affinity energy is :

$$W = \int_\infty^d -\frac{e^2}{4z^2} dz = \frac{e^2}{4d} = V_{Im} \quad (6)$$

and thus

$$A_{eff} = A + V_{Im} \quad (7)$$

Consequently we can define an effective Coulomb integral U_{eff} by :

$$U_{eff} = U - 2 V_{Im} \quad (8)$$

In a very qualitative way and taking into account that physically we must have $A_{eff} < I_{eff}$, three cases can be distinguished according to the value of the metal work function :

(i) $I - \frac{e^2}{4d} > \phi > A + \frac{e^2}{4d}$ i. e. the Fermi level lies between the effective affinity and ionization levels, in these conditions the adatom tends to remain neutral (see Fig. 4) since the transfer of an electron to or from the metal would cost some energy

(ii) $\frac{I+A}{2} < I - \frac{e^2}{4d} < \phi$ i. e. the effective ionization level is above the Fermi level of the metal. The adatom tends to become a positively charged ion since one gains the energy $\phi - I_{eff}$ when transferring an electron from the adatom to the metal.

(iii) $\phi < A + \frac{e^2}{4d} < \frac{I+A}{2}$ i. e. the effective affinity level is below the Fermi energy of the metal. The adatom tends to become a negatively charged ion since one gains the energy $A_{eff} - \phi$ when transferring an electron from the metal to the adatom.

When the adatom comes near the surface, the classical image theory starts to break down and, in addition to their shifts, the levels begin to broaden and therefore the charge transfer may be a fraction of an electron. We

will see in the following that the exact determination of the charge transfer is very difficult since it involves the treatment of electronic interactions. This is a many body problem for which only very approximate solutions exist up to now. This range of distances is actually the most interesting since it corresponds to the distances involved in chemisorption phenomena. The aim of these lectures is to show that, in spite of the difficulties arising from the charge transfer problem, one can set up simple models from which experimental trends can be understood.

3 - ANDERSON-GRIMLEY-NEWNS HAMILTONIAN

The Hamiltonian has been first introduced by Anderson⁽¹⁴⁾ to treat dilute impurity problems in bulk metals. It has been adapted by Grimley⁽¹⁵⁾ and Newns⁽¹⁶⁾ to study the chemisorption of adatoms on a metal surface. Since these early works, this type of Hamiltonian has been used by many others.

The Hamiltonian can be written :

$$H = H_{\text{ads}} + H_{\text{subs}} + H_{\text{coupling}} \quad (9)$$

H_{ads} , H_{subs} and H_{coupling} are respectively the adsorbate, substrate and coupling hamiltonians. For the sake of simplicity, let us consider that only one valence orbital of the adatom is involved in the bonding like in the hydrogen case. Then :

$$H_{\text{ads}} = \sum_{\sigma} \left[\epsilon_a^0 n_{a\sigma} + \frac{1}{2} U n_{a\sigma} n_{a-\sigma} \right] \quad (10.a)$$

$$H_{\text{subs}} = \sum_{k\sigma} \epsilon_k n_{k\sigma} \quad (10.b)$$

$$H_{\text{coupling}} = \sum_{k\sigma} \left[V_{ak} c_{a\sigma}^* c_{k\sigma} + V_{ka} c_{k\sigma}^* c_{a\sigma} \right] \quad (10.c)$$

ϵ_a^0 is the atomic level of the considered atomic orbital $|a\rangle$ and ϵ_k are the eigenvalues of H_{subs} . $c_{a\sigma}^*(c_{a\sigma})$ and $c_{k\sigma}^*(c_{k,\sigma})$ are respectively creation (annihilation) operators in the spin-orbital $|a\sigma\rangle$ and metal state $|k\sigma\rangle$, the corresponding occupation number operators are :

$$n_{a\sigma} = c_{a\sigma}^* c_{a\sigma} \quad (11.a)$$

$$n_{k\sigma} = c_{k\sigma}^* c_{k\sigma} \quad (11.b)$$

U is an effective Coulomb integral on the adatom ($U = I_{\text{eff}} - A_{\text{eff}}$) and is usually taken as a parameter. Finally

$$V_{ak} = \langle a | H | k \rangle = V_{ka}^* \quad (12)$$

is the coupling matrix element. Let us notice that this hamiltonian does not take into account the core-core repulsion between the adatom and substrate atoms.

3 - 1. Hartree-Fock treatment

In the Hartree-Fock approximation the two body operator $n_{a\sigma} n_{a-\sigma}$ is replaced by an effective one body operator :

$$n_{a\sigma} n_{a-\sigma} \Rightarrow \langle n_{a\sigma} \rangle n_{a-\sigma} + \langle n_{a-\sigma} \rangle n_{a\sigma} - \langle n_{a\sigma} \rangle \langle n_{a-\sigma} \rangle$$

In this approximation, H becomes :

$$H = \sum_{\sigma} \left[H_{\text{HF}}^{\sigma} - \frac{1}{2} U \langle n_{a\sigma} \rangle \langle n_{a-\sigma} \rangle \right] \quad (13)$$

with :

$$H_{\text{HF}}^{\sigma} = \epsilon_{a\sigma} n_{a\sigma} + \sum_k \epsilon_k n_{k\sigma} + \sum_k (V_{ak} c_{a\sigma}^* c_{k\sigma} + \text{h.c.}) \quad (14.a)$$

and

$$\epsilon_{a\sigma} = \epsilon_a^0 + U \langle n_{a-\sigma} \rangle \quad (14.b)$$

One sees at first glance that spins are now decoupled and therefore each spin can be treated separately. However since $\epsilon_{a\sigma}$ depends on $\langle n_{a-\sigma} \rangle$, the final solutions should obey a self-consistency condition.

3 - 1. 1. Local density of states on the adsorbate

Let us consider the states with spin σ and assume that $|a\sigma\rangle$, $|k\sigma\rangle$ is a complete orthonormal basis. The local density of states on the adsorbate can be obtained from the corresponding diagonal matrix element of the Green operator :

$$\rho_a^{\sigma}(E) = -\frac{1}{\pi} \lim_{\epsilon \rightarrow 0^+} \text{Im } G_{aa}^{\sigma\sigma}(E + i\epsilon) \quad (15.a)$$

with

$$G_{aa}^{\sigma\sigma}(E + i\epsilon) = \langle a\sigma | \frac{1}{E + i\epsilon - H_{HF}^{\sigma}} | a\sigma \rangle \quad (15.b)$$

$$(E + i\epsilon - H_{HF}^{\sigma})^{-1} = \begin{bmatrix} E + i\epsilon - \epsilon_{a\sigma} & -V_{ak_1} & -V_{ak_2} & \dots \\ -V_{ak_1}^* & E + i\epsilon - \epsilon_{k_1} & 0 & \dots \\ -V_{ak_2}^* & 0 & E + i\epsilon - \epsilon_{k_2} & \dots \\ \vdots & \vdots & \vdots & \ddots \end{bmatrix}^{-1} \quad (16)$$

$G_{aa}^{\sigma\sigma}(E + i\epsilon)$ is the first element of this matrix, i. e. :

$$G_{aa}^{\sigma\sigma}(E + i\epsilon) = \frac{\pi (E + i\epsilon - \epsilon_k)}{(E + i\epsilon - \epsilon_{a\sigma}) \pi (E + i\epsilon - \epsilon_k) - \sum_k |V_{ak}|^2 \pi_{k' \neq k} (E + i\epsilon - \epsilon_{k'})} \quad (17)$$

or equivalently :

$$G_{aa}^{\sigma\sigma}(E + i\epsilon) = \frac{1}{E + i\epsilon - \epsilon_{a\sigma} - \sum_k \frac{|V_{ak}|^2}{E - \epsilon_k + i\epsilon}} = \frac{1}{E + i\epsilon - \epsilon_{a\sigma} - S(E + i\epsilon)} \quad (18)$$

which defines the S function.

Using the well known identity :

$$\lim_{\epsilon \rightarrow 0^+} \sum_k \frac{|V_{ak}|^2}{E - \epsilon_k + i\epsilon} = \mathcal{P} \left[\sum_k \frac{|V_{ak}|^2}{E - \epsilon_k} \right] - i\pi \sum_k |V_{ak}|^2 \delta(E - \epsilon_k) \quad (19)$$

in which \mathcal{P} means the principal part, we can define two functions :

$$\Lambda(E) = \mathcal{P} \left[\sum_k \frac{|V_{ak}|^2}{E - \epsilon_k} \right] \quad (20.a)$$

$$\Delta(E) = \pi \sum_k |V_{ak}|^2 \delta(E - \epsilon_k) \quad (20.b)$$

$$S(E + i0) = \Lambda(E) - i\Delta(E) \quad (20.c)$$

$\Lambda(E)$ and $\Delta(E)$ are not independent but are related through an Hilbert transform :

$$\Lambda(E) = \frac{\mathcal{P}}{\pi} \int_{-\infty}^{+\infty} \frac{\Delta(E')}{E - E'} dE' \quad (21)$$

Consequently :

$$\lim_{\epsilon \rightarrow 0^+} G_{aa}^{\sigma\sigma}(E + i\epsilon) = \frac{1}{E - \epsilon_{a\sigma} - \Lambda(E) + i\Delta(E)} \quad (22)$$

is fully determined by the knowledge of $\Delta(E)$ which is usually called the chemisorption function. From eq. (22) we have :

$$\rho_a^{\sigma}(E) = \frac{1}{\pi} \frac{\Delta(E)}{(E - \epsilon_{a\sigma} - \Lambda(E))^2 + \Delta^2(E)} \quad (23)$$

As already stated $\epsilon_{a\sigma}$ and thus $\rho_a^{\sigma}(E)$ are functions of $\langle n_{a-\sigma} \rangle$ and therefore :

$$\langle n_{a\sigma} \rangle = \int_0^{E_F} \rho_a^{\sigma}(E) dE = N(\langle n_{a-\sigma} \rangle) \quad (24)$$

Therefore the self-consistent $\rho_a^{\sigma}(E)$ should be such as :

$$\langle n_{a-\sigma} \rangle = N(\langle n_{a\sigma} \rangle) = N(N(\langle n_{a-\sigma} \rangle)) \quad (25)$$

Let us discuss the features of $\rho_a^{\sigma}(E)$, assuming that the self-consistent value of $\langle n_{a-\sigma} \rangle$ is known. $\rho_a^{\sigma}(E)$ has a continuous spectrum which comes from $\Delta(E)$ and thus coincides with the substrate energy band. In addition one or two bound states may appear when the equation :

$$E - \epsilon_{a\sigma} - \Lambda(E) = 0 \quad (26)$$

has roots $E_{\ell\sigma}$ outside the continuous spectrum ($\Delta(E) = 0$). The weight of this bound state is given by :

$$\langle n_{\ell\sigma} \rangle = [1 - \Lambda'(E_{\ell\sigma})]^{-1} \quad (27)$$

where $\Lambda'(E) = \frac{d\Lambda(E)}{dE}$. This last quantity is always negative outside the band so that :

$$0 < \langle n_{\ell\sigma} \rangle < 1$$

To proceed further let us adopt a specific form of $\Delta(E)$. Following

News⁽¹⁶⁾, let us replace $|v_{ak}|^2$ by an average value $|v_{ak}|^2_{av}$:

$$\Delta(E) \approx \pi |v_{ak}|^2_{av} \sum_k \delta(E - E_k) \quad (28.a)$$

$$\approx \pi |v_{ak}|^2_{av} \rho(E) \quad (28.b)$$

$\rho(E)$ being the (bulk) substrate density of states which we assume to have a semi-elliptic shape. It is known that this is actually the local density of states on the first atom of a half infinite linear chain in the tight-binding approximation with nearest neighbour hopping integrals (see Appendix 1). Then $\Lambda(E)$ and $\Delta(E)$ are given respectively by the real and imaginary parts of the corresponding Green function multiplied by $|v_{ak}|^2_{av}$. This Green function is derived in Appendix 1 :

$$G(z) = \frac{z \pm \eta \sqrt{z^2 - \frac{W^2}{4}}}{\frac{W^2}{8}} \quad \eta = \pm 1 \quad (29)$$

where W is the bandwidth, the value of η being chosen so that $G(z)$ has the correct behaviour at infinity and has a negative imaginary part. Thus

- if $E < -\frac{W}{2}$

$$\Lambda(E) = |v_{ak}|^2_{av} \frac{E + \sqrt{E^2 - \frac{W^2}{4}}}{\frac{W^2}{8}} \quad (30.a)$$

$$\Delta(E) = 0 \quad (30.b)$$

- if $-\frac{W}{2} < E < \frac{W}{2}$

$$\Lambda(E) = \frac{8E}{W^2} \quad (31.a)$$

$$\Delta(E) = |v_{ak}|^2_{av} \frac{8}{W^2} \sqrt{\frac{W^2}{4} - E^2} \quad (31.b)$$

- if $E > \frac{W}{2}$

$$\Lambda(E) = |v_{ak}|^2_{av} \frac{E - \sqrt{E^2 - \frac{W^2}{4}}}{\frac{W^2}{8}} \quad (32.a)$$

$$\Delta(E) = 0 \quad (32.b)$$

The variations of $\Lambda(E)$ and $\Delta(E)$ with E are shown in Fig. 6. Let us now discuss the two limiting cases :

3 - 1. 1. a) Weak-coupling limit.

This is the case when $|v_{ak}|^2_{av}$ is small compared to W^2 and then $\Delta(E)$ and $\Lambda(E)$ are small compared to W . $\rho_a^{\sigma}(E)$ reaches only a high value when $E = \epsilon_{ao}$ - $\Lambda(E)$ vanishes. This can be solved graphically (Fig. 6.a), one obtains a unique solution :

$$E \approx \epsilon_{ao} + \Lambda(\epsilon_{ao}) \quad (33)$$

If this energy falls within the energy band of the metal, Δ is not zero and can be approximated by $\Delta(\epsilon_{ao})$ in which case the adatom level can be thought of as a virtual bound state with a half width at half maximum (FWHM) $\Delta(\epsilon_{ao})$. If this value of energy falls outside the metal band $\rho_a^{\sigma}(E)$ will be composed of a true bound state E_{eo} with a weight $\langle n_{eo} \rangle$ given by eq. (27) and of a continuous contribution extending all over the metal band with a weight $1 - \langle n_{eo} \rangle$ (Fig. 6a').

3 - 1. 1. b) Strong coupling limit

In this case $|v_{ak}|^2_{av}$ is large relative to W^2 and then $\Lambda(E)$ and $\Delta(E)$ are large compared to W . One sees on Fig. 6.b that eq. (26) has generally three roots (at least when ϵ_{ao} is not too far from the center of the metal band) : one in the metal band and the others on both sides of it. $\rho_a^{\sigma}(E)$ has thus two bound states and between them a weak continuous part extending over the metal band (Fig. 6.b'). These two bound states can be thought of as the bonding and the antibonding states of a surface molecule formed by the adatom

and its neighbours. This will be clearly seen below in the tight-binding formalism.

3 - 1. 1. c) Magnetic versus non magnetic solutions

Two types of solutions are possible for eq. (25) :

(i) $\langle n_{ao} \rangle = \langle n_{a-o} \rangle$. this solution always exists and corresponds to a non magnetic adsorbate.

(ii) $\langle n_{ao} \rangle \neq \langle n_{a-o} \rangle$. in this case the adsorbate has a magnetic moment.

When the two types of solutions exist, in principle, the right solution has the lowest energy. For hydrogen, this solution turns out to be magnetic when the coupling is weak enough. However, the Hartree-Fock scheme for the adatom becomes questionable in this limit since U is larger than $\Delta(\epsilon_{ao})$. Then electronic correlations should be taken into account and it is well known that they decrease the tendency to magnetism which is overestimated in the Hartree-Fock scheme.

3 - 1. 1. d) Adsorption on a substrate with a narrow band.

When the substrate has a narrow band (transition metals) one can describe it in the tight-binding approximation. In this case, one obtains more physical insight into the chemisorption function which can be calculated exactly (i. e. without replacing V_{ak} by an average value). For the sake of simplicity, let us first consider a substrate with one s orbital per site. In the tight-binding approximation we can write :

$$|k\rangle = \sum_i a_i(\epsilon_k) |i\rangle \quad (34)$$

$|k\rangle$ is a band state of the semi-infinite crystal and $|i\rangle$ is the atomic orbital centered at site i .

$$V_{ak} = \langle a | H | k \rangle = \sum_i a_i(\epsilon_k) \beta'_{ai} \quad (35)$$

where $\beta'_{ai} = \langle a | H | i \rangle$ is the hopping integral between the adsorbate and substrate site i . Thus

$$\Delta(E) = \pi \sum_{i,j,k} \beta'_{ai} \beta'_{aj}^* a_i(\epsilon_k) a_j^*(\epsilon_k) \delta(E - \epsilon_k) \quad (36)$$

We can limit the interaction to the nearest neighbours of the adsorbate, and when the adsorption geometry is such that all these neighbours are equivalent $\beta'_{ai} = \beta'$ for any i nearest neighbour of a and $\beta'_{ai} = 0$ otherwise. We get :

$$\Delta(E) = \pi \beta'^2 \sum_{i,j} \sum_k a_i(\epsilon_k) a_j^*(\epsilon_k) \delta(E - \epsilon_k) \quad (37)$$

nearest neighbours
of a

Let us now consider several simple geometries occurring for instance on a surface with a square lattice.

- on top position (Fig. 7.a) the adatom has only one neighbour 1 and

$$\Delta(E) = \pi \beta'^2 \sum_k a_1(\epsilon_k) a_1^*(\epsilon_k) \delta(E - \epsilon_k) \quad (38.a)$$

$$= \pi \beta'^2 n_1(E) \quad (38.b)$$

in which $n_1(E)$ is the surface local density of states of the clean substrate. $\Delta(E)$ is thus proportional to this quantity.

- bridge site (Fig. 7.b). The adatom has two neighbours noted by 1 and 2. Let us first introduce the matrix elements G_{ij}^0 of the clean substrate Green function.

$$G_{ij}^0 = \sum_k \frac{\langle i | k \rangle \langle k | j \rangle}{E + i\epsilon - \epsilon_k} = \sum_k \frac{a_i(\epsilon_k) a_j^*(\epsilon_k)}{E + i\epsilon - \epsilon_k} \quad (39)$$

Consequently

$$\lim_{\epsilon \rightarrow 0^+} \text{Im} G_{ij}^0 = -\pi \sum_k a_i(\epsilon_k) a_j^*(\epsilon_k) \delta(E - \epsilon_k) \quad (40)$$

and

$$\Delta(E) = -\beta'^2 \text{Im} [G_{11}^0 + G_{12}^0 + G_{21}^0 + G_{22}^0] \quad (41)$$

which can be simplified by introducing the group orbital⁽¹⁰⁾

$$|g_s^b\rangle = \frac{1}{\sqrt{2}} (|1\rangle + |2\rangle) \quad (42)$$

$$\Delta(E) = -2\beta'^2 \text{Im} \langle g_s^b | G^0 | g_s^b \rangle \quad (43.a)$$

$$= 2\pi\beta'^2 n_{g_s^b}(E) \quad (43.b)$$

where $n_{g_s^b}(E)$ is the local density of states of the clean substrate associated with the group orbital $|g_s^b\rangle$

- centered site (Fig. 7.c), similarly one obtains :

$$\Delta(E) = 4\pi\beta'^2 n_{g_s^c}(E) \quad (44)$$

with $|g_s^c\rangle = \frac{1}{2}(|1\rangle + |2\rangle + |3\rangle + |4\rangle)$.

Therefore in the general case in which the adsorbate has Z_s equivalent nearest neighbours, $\rho_a^\sigma(E)$ is given by⁽¹⁷⁾ :

$$\rho_a^\sigma(E) = \frac{Z_s \beta'^2 n_{g_s}(E)}{(E - \epsilon_{a\sigma} - Z_s \beta'^2 R_{g_s}(E))^2 + \pi^2 Z_s^2 \beta'^4 n_{g_s}^2(E)} \quad (45)$$

$R_{g_s}(E)$ is the Hilbert transform of $n_{g_s}(E)$ i. e.

$$R_{g_s}(E) = \text{Re} \langle g_s | G^0 | g_s \rangle \quad (46)$$

The state $|g_s\rangle$ is the group orbital associated to the adsorption site i. e. the symmetric linear combination (normalised) of substrate atomic orbitals centered on the nearest neighbours of the adsorbate.

In order to illustrate the preceding calculations let us consider a non magnetic adatom at on top position on the (100) plane of a simple cubic lattice and assume, for simplicity, that $\epsilon_{a\sigma} = \epsilon_a$ coincides with the center of the substrate band.

The corresponding $\rho_a(E)$ are given in Fig. 8 as a function of β'/β , β being the substrate hopping integral. One sees that :

(i) when $\beta' \lesssim \beta$, $\rho_a(E)$ has the shape of a virtual bound state centered at ϵ_a (since $R_{g_s}(E)$ is an odd function) with a half mean width of order $\pi\beta'^2 n_{g_s}(0)$.

(ii) when $\beta' \gtrsim \beta$, $\rho_a(E)$ is composed of two virtual bound states which become true bound states beyond a critical value of $\beta'/\beta \approx 5.35$. These two bound states are actually the bonding and antibonding states of the molecule formed by the adatom and its substrate neighbour weakly perturbed by the "indented" solid.

The case of adsorption on bridge and centered sites is slightly more intricate since the corresponding densities of states associated with the groupe orbital are asymmetric. The qualitative behaviour is the same except that bonding and antibonding bound states appear successively and for lower values of β'/β .

The concept of group orbital can be easily generalised to the case of substrates with degenerate atomic levels and when the atomic level of the adatom is itself degenerate : a group orbital must be associated to each adatom atomic orbital, this group orbital being defined as⁽¹⁶⁾⁽¹⁸⁾

$$|g_{s\lambda}\rangle = A \sum_{i,v} \beta_{ia}^{v\lambda} |iv\rangle \quad \begin{matrix} \lambda = 1, L_a \\ v = 1, L_s \end{matrix} \quad (47)$$

L_a and L_s being respectively the degeneracy of the atomic level of the adatom and the substrate, $\beta_{ia}^{v\lambda}$ are the hopping integrals :

$$\beta_{ia}^{v\lambda} = \langle iv | H | a\lambda \rangle \quad (48)$$

between the adatom and its substrate neighbour i. A is the normalisation factor :

$$A = \left\{ \sum_{i,v} |\beta_{ia}^{v\lambda}|^2 \right\}^{-1/2} \quad (49)$$

However the partial density of states on the adatom $\rho_a^\lambda(E)$ corresponding to orbital λ does not usually take a simple form similar to eq. (45). Nevertheless its general shape is still governed not only by the values of the hopping integrals but also by the adatom coordination number and the surface density of states around the adatom atomic level. Consequently, for a given adsorbate-substrate system, the effective coupling may be weak or strong

according to the surface crystallographic orientation. A typical example is shown in Fig. 9⁽¹⁹⁾ : the coupling of a Mo adatom is weak on Mo(110) ($Z_s = 2$, $n_s(\epsilon_a)$ small) and strong on Mo(100) ($Z_s = 4$, $n_s(\epsilon_a)$ large).

Let us remark that within the tight-binding basis, H_{coupling} takes a simple form. Indeed, for an adsorbate with only one orbital (for simplicity) :

$$\begin{aligned} V_{ak} &= \sum_{j\lambda} \langle a | H | j\lambda \rangle \langle j\lambda | k \rangle \\ c_k &= \sum_{1v} \langle k | 1v \rangle c_{1v} \end{aligned} \quad (50)$$

$$\begin{aligned} \sum_k V_{ak} c_a^\dagger c_k &= \sum_{j\lambda} \langle a | H | j\lambda \rangle \underbrace{\sum_{k,1v} \langle j\lambda | k \rangle \langle k | 1v \rangle}_{\delta_{1j} \delta_{\lambda v}} c_a^\dagger c_{1v} \\ &= c_a^\dagger \sum_{1v} \langle v | H | a \rangle^* c_{1v} \\ &= A^{-1} c_a^\dagger c_g \end{aligned} \quad (51)$$

c_{g_s} being the annihilation operator of the group orbital $|g_s\rangle$

Thus

$$H_{\text{coupling}} = A^{-1} (c_a^\dagger c_{g_s} + c_{g_s}^\dagger c_a) \quad (52)$$

3 - 1. 2. Binding energy.

The binding energy E_B of the adsorbate is the difference between the total energy of the semi-infinite crystal with the adsorbed atom and that of the same system with the adatom infinitely far from the surface.

Let us now show that this binding energy is fully determined by the knowledge of the chemisorption function $\Delta(E)$. If one neglects the core-core repulsion between the adsorbate and the substrate atoms, this energy can be written :

$$E_B = \int_{-\infty}^{E_F + \delta E_F} E N'(E) dE - \int_{-\infty}^{E_F} E N(E) dE - \epsilon_a^0 - U \langle n_{a\sigma} \rangle \langle n_{a-\sigma} \rangle \quad (53)$$

$N'(E)$ is the total density of states of the semi-infinite crystal with the adsorbed atom and $N(E)$ the total density of states of the clean semi-infinite crystal. Thus $N'(E)$ is normalised to $N + 1$ atoms and $N(E)$ to N atoms. The first three terms account for the variation of the total one-electron energy when the adatom is brought from infinity and the last term avoids the double counting of the electronic interactions in the Hartree scheme (see eq. 13). In order to ensure the conservation of the total charge, it is necessary to allow a small (but unphysical) variation of the Fermi level. This point will be discussed later with more details.

Then eq. (53) can be transformed into :

$$E_B = \int_{-\infty}^{E_F} E \Delta N(E) dE + E_F N'(E_F) \delta E_F - \epsilon_a^0 - U \langle n_{a\sigma} \rangle \langle n_{a-\sigma} \rangle \quad (54)$$

with $N'(E) - N(E) = \Delta N(E)$.

The charge conservation can be written :

$$\int_{-\infty}^{E_F + \delta E_F} N'(E) dE - \int_{-\infty}^{E_F} N(E) dE = 1 \quad (55)$$

or

$$\int_{-\infty}^{E_F} \Delta N(E) dE + N'(E_F) \delta E_F = 1 \quad (56)$$

where we have assumed that the adatom valence orbital is occupied in the free state by one electron.

The binding energy thus becomes :

$$E_B = \int_{-\infty}^{E_F} (E - E_F) \Delta N(E) dE + E_F - \epsilon_a^0 - U \langle n_{a\sigma} \rangle \langle n_{a-\sigma} \rangle \quad (57)$$

As shown in Appendix 2, the variation of the total density of states when the Hamiltonian H_0 is changed into $H_0 + V$ is given by

$$\Delta n(E) = \mp \frac{1}{\pi} \text{Im} \frac{d}{dE} \text{Log Det}(1 - VG^{\sigma\pm}) \quad (58)$$

where $G^{0\pm} = (E - H_0 \pm i\epsilon)^{-1}$ and $H_0 = \sum_{\sigma} \epsilon_{a\sigma} n_{a\sigma} + \sum_k \epsilon_k n_{k\sigma}$.

V is the coupling between the adatom and the substrate and then :

$$\Delta n(E) = \Delta N(E) - \sum_{\sigma} \delta(E - \epsilon_{a\sigma}) \quad (59)$$

Let us calculate $\text{Det}(1 - VG^{0\pm})$. This determinant factorizes into two determinants, one for each spin, having the following form :

$$\begin{vmatrix} 1 & -V_{ak_1} G_{k_1 k_1}^{0\pm} & -V_{ak_2} G_{k_2 k_2}^{0\pm} & \dots \\ -V_{k_1 a} G_{aa}^{0\pm} & 1 & 0 & \\ -V_{k_2 a} G_{aa}^{0\pm} & 0 & 1 & \\ \vdots & \vdots & \vdots & \ddots \end{vmatrix} \quad (60)$$

Thus

$$\text{Det}(1 - VG^{0\pm}) = \prod_{\sigma} \left[1 - \sum_k |V_{ak}|^2 G_k^{0\pm} G_{aa}^{0\pm} \right] \quad (61)$$

Replacing $G_{kk}^{0\pm}$ and $G_{aa}^{0\pm}$ by their expressions one finds :

$$\text{Det}(1 - VG^{0\pm}) = \prod_{\sigma} \left[\sum_k \frac{|V_{ak}|^2}{k(E \pm i\epsilon - \epsilon_{a\sigma})(E \pm i\epsilon - \epsilon_k)} \right] \quad (62.a)$$

$$= 1 - \frac{1}{E \pm i\epsilon - \epsilon_{a\sigma}} S(E \pm i\epsilon) \quad (62.b)$$

and eq. (58) leads to :

$$\Delta n(E) = \sum_{\sigma} \mp \frac{1}{\pi} \text{Im} \frac{d}{dE} \text{Log}(E - \epsilon_{a\sigma} - S(E \pm i\epsilon)) - \delta(E - \epsilon_{a\sigma}) \quad (63)$$

thus

$$\Delta N(E) = \sum_{\sigma} \mp \frac{1}{\pi} \text{Im} \frac{d}{dE} \text{Log}(E - \epsilon_{a\sigma} - S(E \pm i\epsilon)) \quad (64.a)$$

$$= \sum_{\sigma} \mp \frac{1}{\pi} \text{Im} \frac{d}{dE} \text{Log} \left\{ G_{aa}^{0\pm}(E) \right\}^{-1} \quad (64.b)$$

$$= \sum_{\sigma} \mp \frac{1}{\pi} \lim_{\epsilon \rightarrow 0^+} \text{Im} \left[1 - \frac{dS(E \pm i\epsilon)}{dE} \right] G_{aa}^{0\pm}(E) \quad (64.c)$$

Let us define $\Delta N(E)$:

$$\Delta N(E) = \int_{-\infty}^{E_F} \Delta N(E) dE \quad (65)$$

then integrating by parts using eq. (64.b) with $G_{aa}^{0\pm}(E)$

$$\int_{-\infty}^{E_F} (E - E_F) \Delta N(E) dE = - \int_{-\infty}^{E_F} \Delta N(E) dE \quad (66.a)$$

$$= \sum_{\sigma} \left[E_{\ell\sigma} + \frac{1}{\pi} \int_m^{E_F} \text{Im} \text{Log}(E - \epsilon_{a\sigma} - \Lambda(E) + i\Delta(E)) dE \right] \quad (66.b)$$

in which $E_{\ell\sigma}$ is the bound state with spin σ (when existing) and m is the bottom of the substrate band.

Finally :

$$E_B = \sum_{\sigma} \left[E_{\ell\sigma} + \frac{1}{\pi} \int_m^{E_F} \text{arctg} \frac{\Delta(E)}{E - \epsilon_{a\sigma} - \Lambda(E)} dE \right] + E_F - \epsilon_a^0 - U \langle n_{a\sigma} \rangle \langle n_{a-\sigma} \rangle \quad (67)$$

with

$$0 < \text{arctg} x < \pi$$

when there is an occupied bound state and

$$-\pi < \text{arctg} x < 0 \text{ otherwise.}$$

With this formula News⁽¹⁶⁾ has calculated the chemisorption energy of hydrogen on Ti, Cr, Ni and Cu as a function of the coupling strength and the corresponding charge transfer. Although the sign of the charge transfer agrees with experiments (variation of the work function during adsorption or more recently variation of core level binding energy of the substrate surface atoms), its order of magnitude is too large. This formalism had also previously been used by Grimley⁽¹⁸⁾ to study the indirect (i. e. via the substrate) interaction between two adatoms.

3 - 1. 3. Discussion

We have already mentioned two weak points of this formalism : one must assume a non physical variation of the Fermi level to ensure the total charge neutrality and magnetic solutions are too easily obtained. Actually, a proper treatment should obey the Friedel sum rule⁽²⁰⁾ i. e. :

$$\int_{-\infty}^{E_F} \Delta N(E) dE = 1 \quad (68)$$

which is generally not fulfilled by $\Delta N(E)$ given by eq. (64). Concerning the second point, the Hartree-Fock treatment implicitly assumes that U is small compared to the mean width of $\rho_a^\sigma(E)$, it allows any charge fluctuation as in any molecular orbital (MO) approach. The effect of Coulomb electronic interactions is only treated to the first order and thus an obvious improvement would be to go at least to second order. Such improved models have been proposed by several authors, they will be briefly discussed in the next section. On the other hand, for some transition metals, the effective Coulomb integral of the substrate may be important.

3 - 2. Beyond the Hartree-Fock treatment.

Since the first works based on the Hartree-Fock approximation we have described in the preceding sections, many attempts have been made to improve this treatment by including many body effects. Many of them aimed at a better description of the one particle spectrum of the adsorbate⁽²¹⁻²⁶⁾. As far as the total energy is concerned, although the general formula derived by Kj  llerstr  m et al.⁽²⁷⁾ for the dilute impurity problem can be used to compute the binding energy of a chemisorbed atom, few authors did calculate this quantity⁽²⁸⁾⁽²⁹⁾.

We have seen that in the Hartree-Fock treatment all the interesting physical properties of the chemisorbed system can be derived from the knowledge of the Green function $G_{aa}^{\sigma\sigma}$ of the adsorbate (see eqs. (64.b) and (67)). This fact remains true when many-body effects are taken into account. In these lecture notes we will not give the exact derivation which can be found in Kj  llerstr  m et al.⁽²⁷⁾ but we will rather generalize in an intuitive way eq. (22) for the Green function and eq. (57) for the binding energy.

In the expression of $G_{aa}^{\sigma\sigma}$, the introduction of the adsorbate Coulomb interaction gives rise to a self energy $\Sigma_{a\sigma}$ which, in the Hartree-Fock scheme is nothing but $U \langle n_{a-\sigma} \rangle$ (eq. (14.b)). In the general case $\Sigma_{a\sigma}$ becomes a complex function of the energy and eq. (22) is now written :

$$\lim_{\epsilon \rightarrow 0^+} G_{aa}^{\sigma\sigma}(E + i\epsilon) = \frac{1}{E - \epsilon_a^0 - \Sigma_{a\sigma}(E + i\epsilon) - \Lambda(E) + i\Delta(E)} \quad (69)$$

from which one derives the one particle excitation spectrum of the adsorbate by eq. 15.a.

To generalize the expression of the binding energy let us rewrite eq. (57). The first term can be transformed into a contour integral (see Appendix 3) in which the causal Green function on the adsorbate appears

$$c_{G_{aa}^{\sigma\sigma}}(E) = \frac{1}{E - \epsilon_a^0 - U \langle n_{a-\sigma} \rangle - S(E)} \quad (70)$$

with

$$S(E) = \sum_k \frac{|v_{ak}|^2}{E - \epsilon_k + i\eta \operatorname{sgn}(E - E_F)}$$

then

$$\int_{-\infty}^{E_F} (E - E_F) \Delta N(E) dE = \frac{1}{2\pi i} \int_C \int_{-\infty}^{\infty} (z - E_F) \left(1 - \frac{dS}{dz}\right) c_{G_{aa}^{\sigma\sigma}}(z) dz \quad (71)$$

where C is the contour consisting of the real axis and a semi-circle at infinity in the upper half plane.

The last term in eq. (57) can also be written as a contour integral :

$$U \langle n_{a-\sigma} \rangle \langle n_{a\sigma} \rangle = \frac{1}{4\pi i} \int_C \int_{-\infty}^{\infty} \Sigma_{a\sigma}^{\text{HF}} c_{G_{aa}^{\sigma\sigma}}(z) dz \quad (72)$$

where

$$\Sigma_{a\sigma}^{\text{HF}} = U \langle n_{a-\sigma} \rangle$$

Finally, the expression of the adsorption energy in the Hartree-Fock approximation becomes :

$$E_B = \frac{1}{2\pi i} \int_C (z - E_F) \left(1 - \frac{dS}{dz}\right) c_{Gaa}^{\sigma\sigma}(z) dz - \frac{1}{4\pi i} \int_C \sum_{\sigma}^{\text{HF}} \Sigma_{a\sigma}^{\text{HF}}(z) c_{Gaa}^{\sigma\sigma}(z) dz - (\epsilon_a^0 - E_F) \quad (73)$$

One can show that this equation remains valid in the general case if one replaces in eq. (73), $\Sigma_{a\sigma}^{\text{HF}}$ by $\Sigma_{a\sigma}(z)$. Thus the problem reduces to the determination of $\Sigma_{a\sigma}(z)$. Expressions of $\Sigma_{a\sigma}(z)$ exist only in different limits :

i) if $U \rightarrow 0$, one can use a second order perturbation theory in $U/W^{(23)(30)}$, W being the broadening of the adatom level. One finds :

$$\Sigma_{a\sigma}(z) = \Sigma_{a\sigma}^{\text{HF}} + U^2 \int_{-\infty}^{E_F} dE_2 \int_{E_F}^{\infty} dE_3 \int_{E_F}^{\infty} dE_4 \frac{\rho_a^{-\sigma}(E_2) \rho_a^{-\sigma}(E_3) \rho_a^{-\sigma}(E_4)}{z + E_2 - E_3 - E_4} + U^2 \int_{E_F}^{\infty} dE_2 \int_{-\infty}^{E_F} dE_3 \int_{-\infty}^{E_F} dE_4 \frac{\rho_a^{-\sigma}(E_2) \rho_a^{-\sigma}(E_3) \rho_a^{-\sigma}(E_4)}{z + E_2 - E_3 - E_4} \quad (74)$$

ii) when the coupling $V = 0$, one can write an exact expression for $c_{Gaa}^{\sigma\sigma}$:

$$c_{Gaa}^{\sigma\sigma} = \frac{\langle n_{a-\sigma} \rangle}{\omega - \epsilon_a^0 - U} + \frac{1 - \langle n_{a-\sigma} \rangle}{\omega - \epsilon_a^0} \quad (75)$$

which is rather intuitive since the first term has a pole at the affinity level with a weight $\langle n_{a-\sigma} \rangle$ and the other at the ionisation level with a weight $1 - \langle n_{a-\sigma} \rangle$. The above equation defines $\Sigma_{a\sigma}(z)$ since G be identified with the expression

$$G = \frac{1}{E - \epsilon_a^0 - U \langle n_{a-\sigma} \rangle - \Sigma_{a\sigma}(z)} \quad (76)$$

thus

$$\Sigma_{a\sigma}(z) = \frac{\langle n_{a-\sigma} \rangle \langle n_{a\sigma} \rangle U^2}{z - \epsilon_a^0 - U \langle n_{a-\sigma} \rangle} \quad (77)$$

In the general case one should find an interpolation formula between these two limits. Such a formula have been proposed by Martín-Rodero et al. ⁽³¹⁾ and Baldo et al. ⁽²⁴⁻²⁶⁾. Previously several treatments, based on the equations of motion of the Green function, were performed by Brenig and

Schönhammer⁽²¹⁾, Schuck⁽³²⁾, Bell and Madhukar⁽²²⁾. Recently an extensive calculation of the chemisorption energy of H on Ni(100), Ni(111) and W(110) has been done by Piccitto et al. ⁽²⁹⁾. This work uses an approximate self-energy and takes into account the repulsion energy between the hydrogen adatom and the metal. The adatom-substrate coupling parameters are determined as a function of distance through the overlap integrals between the adatom and the metal orbitals as in the extended Hückel method. Finally the variation of U with the adatom distance is parametrized. Then these authors were able to minimized the chemisorption energy as a function of the position of the adatom. Although the treatment of the electronic structure of the metal is strongly simplified (semi-elliptical density of states) the results seem to be in fair agreement with more sophisticated schemes.

In conclusion, although some improvements have been made to take into account the effect of electronic correlations on the adsorbate, very little is known about the effect of the electronic correlations of the substrate in this context.

4 - A SIMPLE CHEMISORPTION MODEL FOR TIGHT-BINDING SYSTEMS

The Anderson-Grimley-Newns hamiltonian has been mainly used to study the chemisorption of hydrogen on metals, however very few systematic studies of chemisorption on transition metals varying the nature of the adsorbate and substrate can be found in the literature. Moreover, save for the work of Piccitto et al. ⁽²⁹⁾, the position of the adsorbate is assumed to be known. Nevertheless if our goal is to explain all the experimental trends discussed in the introduction, one needs to calculate the binding energy of the adsorbate as a function of its three coordinates from which it is possible to derive the most stable adsorption site and its energy, the bond length, the activation energy for surface diffusion (extrapolated at 0 K) and also vibration frequencies. This calculation should be done for a very large number

of chemisorption systems which obviously is only practically possible if one uses simplified models pointing out the essential physical parameters. Such models have been derived in the framework of the tight-binding formalism for chemisorption on transition metals⁽³²⁻³⁶⁾. In this section we will describe these models and show that they explain, at least semi-quantitatively all the trends observed experimentally.

4 - 1. Models

4 - 1. 1. General characteristics

The binding energy is written :

$$E_B(x, y, z) = \Delta E_b + \Delta E_{rep} + \Delta E_{cor} \quad (78)$$

where ΔE_b , ΔE_{rep} and ΔE_{cor} are respectively the variations of the band, repulsive and Coulomb correlations total energies when the adatom is brought from infinity to the point of coordinates (x, y, z) relative to the surface.

Let us now briefly describe these three contributions.

4 - 1. 1. a) The band contribution

The band contribution ΔE_b is calculated in a tight-binding formalism assuming that the adsorbate-substrate hopping integrals decrease exponentially with distance. The other parameters are the atomic levels of the atoms involved in the chemisorption bond. It is clear that the adsorbate-substrate interactions modify the potential, and then the atomic levels of these atoms. Ideally these potentials and the charge on each atom should be calculated in a self-consistent manner. The simplest assumption is to limit the perturbation of the atomic levels to the adsorbate site. Let us also assume, for simplicity, that the adatom is not magnetic. Then two methods have been used to determine the effective atomic level ϵ_a^M of the adsorbate.

- The Anderson-Grimley-Newns model in which for an H adatom in the Hartree-Fock scheme

$$\epsilon_a^M = \epsilon_a^0 + U \langle n_a \rangle \quad (79)$$

where $\langle n_a \rangle$ is the occupation number per spin orbital. As seen previously, we are obliged in this method to introduce an unphysical variation of the Fermi level in order to ensure the total charge conservation.

- One can also state that the Fermi level should remain unchanged in the chemisorption process and then ϵ_a^M is determined from the Friedel sum rule which can be written (global neutrality condition) :

$$\Delta N(E_F, \epsilon_a^M) = N_a \quad (80)$$

where N_a is the number of valence electrons of the adsorbate involved in the bond. From the knowledge of ϵ_a^M , the charge of any atom of the system can be derived. However numerical calculations have shown that this often leads to a charge transfer on the adatom nearest neighbours which is of the same order of magnitude as on the adatom itself. In these conditions it seems unphysical to neglect the variation of the effective atomic levels of these neighbours. Moreover in some particular cases unphysical charge is found on the adatom which should be strongly reduced if one extends the perturbation of the potential to the nearest neighbours. If this is done on p nearest neighbours, one needs $p + 1$ equations to derive the atomic levels of the adsorbate and its nearest neighbours. Since the Friedel sum rule only brings one equation, one should find new physical conditions.

The simplest condition obeying the Friedel sum rule is to assume that each atom involved in the chemisorption system remains neutral. This condition seems reasonable for many systems, at least at low coverage since work function measurements and 4f surface core level spectroscopy (on 5d elements) are inconsistent with charge transfers larger than 0.1 - 0.2 electrons. This implies that the adsorbate effective atomic level falls in the substrate band since otherwise the charge transfer would be very large.

As in the Anderson-Grimley-Newns model two limits are usually considered

- the weak coupling limit for which adsorbate-substrate integrals are much smaller than the substrate-substrate ones
- the strong coupling limit in the opposite case.

In both cases some band energy is gained ($\Delta E_b < 0$). This contribution is attractive since it is roughly proportional to the adsorbate-substrate hopping integrals which decrease with distance. We will see that it cannot be written as a sum of pair interactions.

4 - 1. 1. b) The repulsive contribution

The repulsive contribution comes mainly from the compression of inner shells. It is written as a sum of phenomenological Born-Mayer pair potentials decreasing exponentially with distance⁽³⁶⁾.

Note that we thus take into account the interaction between the outer valence orbitals of the adsorbate and the d valence electrons of the metal neglecting the role played by the sp electrons of the metal. Indeed these latter electrons give rise to both attractive and repulsive contributions to the binding energy. The repulsive contribution is phenomenologically taken into account in the Born-Mayer potential. Concerning the attractive contribution we assume that the free sp electrons serve primarily to renormalize the hopping parameters. In any case we believe that the sp contribution is rather small in transition metals and thus a treatment which includes only the d band of the metal is satisfactory.

4 - 1. 1. c) The electronic correlation contribution

The contribution of the electronic correlation ΔE_{cor} is obtained from perturbation theory up to the second order in the band limit (intraatomic Coulomb integral small compared to the band width). It includes not only the contribution of the adsorbate as in the Anderson-Grimley-Newns hamiltonian but also the contribution of the substrate. We will see in the following that, to a good approximation, it can be written as a sum of local terms : it

corresponds to an energy gain on the adsorbate and to an energy loss on its neighbours.

4 - 1. 2. Analytical models

We will first use schematical densities of states and neglect the electronic correlation term to be able to derive analytically simple expressions for the chemisorption energy.

4 - 1. 2. a) Weak coupling limit

The band contribution can be split into two terms

$$\Delta E_b = \Delta E_{ba} + \Delta E_{bs} \quad (81)$$

where ΔE_{ba} is the variation of energy due to the broadening of the adsorbate level and ΔE_{bs} is the variation of energy of the substrate due to the adsorption. In the weak coupling limit this last term can be neglected. Then provided that the charge neutrality is ensured i. e. :

$$N_a = L_a \int_{-\infty}^{E_F} n_a(E, \epsilon_a^*) dE \quad (82)$$

ΔE_b takes the form :

$$\Delta E_b = L_a \int_{-\infty}^{E_F} E n_a(E, \epsilon_a^*) dE - N_a \epsilon_a - N_a (\epsilon_a^* - \epsilon_a) \quad (83.a)$$

$$= L_a \int_{-\infty}^{E_F} E n_a(E, \epsilon_a^*) dE - N_a \epsilon_a^* \quad (83.b)$$

where N_a , L_a , n_a , ϵ_a^* , ϵ_a are respectively the number of electrons and the degeneracy in the valence shell of the adsorbate, its local density of states and its atomic level in the adsorbed and free states. The first and second term of eq. (83.a) represent the variation of the one electron energy between the adsorbed state and the free state. The third term represents the variation of the average electronic Coulomb interaction which is counted twice in the first term. If we assume that the local density of states on the adsorbate is rigidly shifted when ϵ_a^* varies, it is straightforward to show that ΔE_b remains constant. Indeed if ϵ_a^* varies by $\delta \epsilon_a^*$, all one electron energies in the first

term vary by $\delta\epsilon_a^M$, thus the total variation is $N_a \delta\epsilon_a^M$ which is exactly cancelled by the variation of the second term.

In the weak coupling limit the broadening of the adatom level is small and the local density of states on the adsorbate exhibits a single peak which can be schematised by a rectangle of width W and centered at ϵ_a^M . The width W_a is chosen so that the centered second moment of the rectangle is equal to the centered second moment of the exact local density of states i. e.

$$\mu_{2a}^c = \int_{-\infty}^{+\infty} (E - \epsilon_a^M)^2 n_a(E, \epsilon_a^M) dE = \frac{1}{W_a} \int_{-\epsilon_a^M/2}^{W_a/2} E^2 dE \quad (84)$$

so that

$$W_a = 2 \sqrt{3} \sqrt{\mu_{2a}^c} \quad (85)$$

μ_{2a}^c can be easily obtained in the tight binding approximation since one can show that :

$$\mu_{2a}^c = \frac{2}{L_a} \sum_{\lambda \neq \mu} \langle \lambda | H | \mu \rangle \langle \mu | H | \lambda \rangle \quad (86)$$

If we assume that the adatom has Z equivalent nearest neighbours we find :

$$\mu_{2a}^c = Z \beta^2 \quad (87)$$

with $\beta^2 = s\sigma^2$ for an adsorbate with an s orbital

$$\beta^2 = \frac{1}{3}(p\sigma^2 + 2pd\pi^2) \text{ for an adsorbate with } p \text{ orbitals}$$

$$\beta^2 = \frac{1}{5}(dd\sigma^2 + 2dd\pi^2 + 2dd\delta^2) \text{ for an adsorbate with } d \text{ orbitals}$$

$s\sigma$, $p\sigma$, $p\pi$, $dd\sigma$, $dd\pi$, $dd\delta$ are the usual Slater-Koster⁽²⁷⁾ hopping integrals between the adatom orbital and the d orbitals of the transition metal substrate. Then the variation with the interatomic distance R can be approximated by an exponential law so that

$$\mu_{2a}^c = Z \beta^2 e^{-2qR} \quad (88)$$

From eq. (82) we get, using the rectangular density of states

$$E_F = \frac{W_a}{L_a} (N_a - \frac{L_a}{2}) \quad (89)$$

Then using eq. (83) we obtain

$$\Delta E_b = \frac{W_a}{2L_a} N_a (N_a - L_a) \quad (90)$$

$$= -\sqrt{Z} B(N_a) e^{-qR} \quad (91)$$

with

$$B(N_a) = \sqrt{3} \frac{|\beta_a'|}{L_a} N_a (N_a - L_a) \quad (92)$$

On the other hand the variation ΔE_{rep} of the repulsive term is given by :

$$\Delta E_{rep} = Z A e^{-pR} \quad (93)$$

where A and p are some given constants.

Finally the binding energy of the adatom with bondlengths R is given by

$$E_B(R) = Z A e^{-pR} - \sqrt{Z} B(N_a) e^{-qR} \quad (94)$$

E_B reaches a minimum if $p > q$ for an equilibrium bond length equal to

$$R_0 = \frac{1}{(2p-q)} \log Z + \frac{1}{p-q} \log \frac{pA}{qB} \quad (95)$$

thus R_0 increases with Z . This fact can be easily understood. Let us consider an adatom with coordination Z , the bond length of which is R_0 . If we increase Z keeping R_0 constant, the repulsive force overcomes the attractive one since this last force varies less rapidly with Z and thus the bond length increases.

If we report eq. (95) into eq. (94) we obtain the binding energy at equilibrium :

$$E_B(R_0) = \left(\frac{q}{p} - 1 \right) B \left(\frac{pA}{qB} \right)^{-q/p-q} Z^{(p-2q)/2(p-q)} \quad (96)$$

Therefore

$$E_B(R_0) \propto Z^\alpha \quad (97)$$

with

$$\alpha = \frac{p-2q}{2(p-q)}$$

For real systems $p > 2q$ and the binding energy increases with Z , therefore the most stable position corresponds to the site with the largest coordination number available on the surface. The latter number being larger on open surfaces than on closed-packed ones, we expect $|E_B|$ to increase when the

density of surface atoms decreases. In realistic cases $\alpha \lesssim \frac{1}{3}$ and consequently the anisotropy of E_B is very much reduced from the value predicted by a broken bond model ($\alpha = 1$) or in a tight-binding scheme with rigid bond lengths ($\alpha = \frac{1}{2}$).

Note that in this model the binding energy is independent of the filling of the substrate band for given A , p , β'_0 and q parameters.

On highly symmetrical surfaces (with low index), the diffusion path can be easily guessed, the bottom of the well and the saddle point corresponding to special symmetry points. Surface diffusion activation energies Q at 0 K are thus given by the difference of binding energy between two sites which differ by their coordination number, the smaller one Z_s corresponding to the saddle point. Then

$$Q = E_B(Z_s) - E_B(Z) = \left[1 - \left(\frac{Z_s}{Z}\right)^\alpha\right] |E_B(Z)| \quad (98)$$

One sees that Q follows the same behaviour as $|E_B|$.

4 - 1. 2. b) Strong coupling limit

In the weak coupling case, we have assumed a rigid local density of states on the adsorbate shifting with E_F in order to conserve the number of electrons on the adatom. In the strong coupling limit, this assumption is no longer valid since the adatom local density of states exhibits two peaks corresponding to the bonding and antibonding states of the "surface molecule". One can predict that their relative weight should be a function of the substrate band filling if the adatom remains neutral. This is pictured in Fig. 10 in which one sees that the weight of the bonding state decreases in favour of the antibonding one when the number of d electrons of the substrate increases. As a consequence and contrary to the weak coupling case, the contribution of the adsorbate to ΔE_B is expected to depend on the position of the Fermi level.

In the following we show using a very simple model that this explains the decrease of the binding energy of N, O, F and H along a transition series. We mimic the adatom local density of states by two δ functions of weights α and $1-\alpha$ at energies $-X$ and X :

$$n_a(E) = \alpha \delta(E + X) + (1 - \alpha) \delta(E - X) \quad (99)$$

The first and second moments of this distribution should be equal respectively to the effective atomic level of the adatom ϵ_a^M and to the second moment of the exact adatom local density of states (i. e. $\mu_2 = Z \beta'^2 + \epsilon_a^{M2}$). These relations fix α and X

$$\alpha = \frac{1}{2} \left[1 - \frac{\epsilon_a^M}{\sqrt{Z \beta'^2 + \epsilon_a^{M2}}} \right] \quad (100)$$

$$X = \sqrt{Z \beta'^2 + \epsilon_a^{M2}}$$

The energy levels are then filled with the N_a electrons of the adsorbate and one finds that the one electron contribution of the adatom to the binding energy is:

$$|E_B| = N_a \sqrt{Z \beta'^2 \frac{1-\alpha}{\alpha}} \quad (101)$$

when all the adatom electrons are in the bonding state ($\alpha > \frac{N_a}{L_a}$) and:

$$|E_B| = (L_a - N_a) \sqrt{Z \beta'^2 \frac{\alpha}{1-\alpha}} \quad (102)$$

when the antibonding state is partially occupied ($\alpha < \frac{N_a}{L_a}$). From these results, one can deduce easily the behaviour of $|E_B|$ as a function of the substrate band filling: knowing that α is a decreasing function of this quantity. One finds that $|E_B|$ reaches a maximum when the bonding state is completely filled and the antibonding one empty which occurs for $\alpha = \frac{N_a}{L_a}$ i. e. at the beginning of the series when $N_a/L_a > \frac{1}{2}$ and at the end when $N_a/L_a < \frac{1}{2}$ and around the middle of the series when $N_a/L_a = 1/2$ (Fig. 11). This explains the

observed decrease of the binding energy of N, O, F and H for substrate starting from the V, Nb and Ta column to the end of the corresponding transition series (Fig. 2).

4 - 1. 3. Improved models

We have just shown that the trends followed by the adsorbate binding energies can be explained using very simple models. It remains to verify that these trends remain valid in a more realistic calculation and for more realistic systems for which the coupling can be intermediate between the two discussed limits. Actually, the calculation of the density of states using a continued fraction technique does not make any assumption on the coupling strength.

Let us recall that in this technique, any diagonal Green function is written as a continued fraction⁽³⁸⁻³⁹⁾,

$$g_{ii}(z) = \frac{1}{z - a_1^i - \frac{b_1^i}{z - a_2^i - \frac{b_2^i}{z - \dots}}} \quad (103)$$

in which the first coefficients a_n^i , b_n^i are calculated exactly. When the spectrum presents no gap, these coefficients converge rapidly and consequently an excellent approximation is obtained by replacing the unknown coefficients by their asymptotic values a_∞ , b_∞ . This is equivalent to terminating the continued fraction by a complex function $F(z)$

$$g_{ii}(z) = \frac{1}{z - a_1^i - \frac{b_1^i}{z - a_2^i - \frac{b_2^i}{z - \dots - a_N^i - b_N^i F(z)}}} \quad (104)$$

$F(z)$ obeys the following quadratic equation

$$F(z) = \frac{1}{z - a_\infty - b_\infty F(z)} \quad (105)$$

and has an imaginary part when the discriminant :

$$D = (z - a_\infty)^2 - 4b_\infty$$

is negative. a_∞ and b_∞ are then related to the band limits m , M by :

$$a_\infty = \frac{m + M}{2} \quad (106)$$

$$b_\infty = \frac{(M - m)^2}{16} = \frac{W^2}{16} \quad (107)$$

where W is the bandwidth.

Let us note that the continued fraction coefficients and the moment of the corresponding local density of states are related and that a continued fraction with N exact levels has $2N$ exact moments. In particular a_1^i is the center of gravity of the local density of states (i. e. the effective atomic level of atom i) and b_1^i is the centered second moment (see eq. 86). Actually this technique, when applied to obtain the adatom local density of states, does not make any assumption on the coupling strength (which is measured by $\sqrt{b_1}$). Consequently it can describe both the weak ($b_1 \ll b_\infty$) and the strong ($b_1 \gg b_\infty$) coupling cases but also all intermediate cases.

We have then developed an improved model in which the local densities of states are obtained from a continued fraction expansion of the Green function exact to the third moment (i. e. with exact a_1 , b_1 , a_2). This has the advantage of giving the correct band limits and asymmetry. On the other hand we now take into account the modification of the substrate electronic structure due to the adsorption. Finally, the calculation is done for a real surface crystalline structure and we are no more restricted to equivalent bonds.

In practice, the perturbation due to the adsorbate extends only over a few sites. Consequently

$$\Delta E_{\text{rep}} = \sum_i A e^{-pR_i} \quad (108)$$

where R_i is the distance between the adatom and the neighbour i .

$$\Delta E_b = \Delta E_{ba} + \sum_i \Delta E_b^i \quad (109)$$

where

$$\Delta E_{ba} = L_a \int_{-\infty}^{E_F} E n_a(E, \dots, \epsilon_j^*) dE - N_a \epsilon_a^* \quad (110)$$

$$\Delta E_b^i = 10 \int_{-\infty}^{E_F} E \delta n_i(E, \dots, \epsilon_j^*) dE - N_s \delta \epsilon_i^* \quad (111)$$

are respectively the adsorbate and substrate atom i contributions to the band part of the binding energy. In eqs. (108) and (109) the sum over i is limited to the perturbed atoms. All the effective atomic levels ϵ_j^* are determined by requiring that all atoms (adatom and substrate neighbours) remain neutral. Finally δn_i and $\delta \epsilon_i^*$ are respectively the variation of the local density of states and effective atomic level on atom i due to the adsorption.

Let us now discuss the electronic correlation term. If we neglect the electronic correlations in the substrate, we could start with eq. 73 using for the self-energy the expression (74), but since we have assumed that the effective atomic levels can be fixed by a local charge neutrality condition and not by eq. (79) such a treatment would be inconsistent. Moreover, since we want to take into account the Coulomb interaction in the metal, eq. (73) can no more be used. To describe the Coulomb correlations in the metal, let us add to the Anderson-Grimley-Newns hamiltonian a Hubbard term :

$$H_{\text{Hub}} = \frac{U}{2} \sum_i \left[1 - \delta_{vv'} \delta_{\sigma\sigma'} \right] n_{iv\sigma} n_{iv'\sigma'} \quad (112)$$

where $n_{iv\sigma}$ is the occupation number operator of orbital v centred at site i with spin σ . Since we are interested in the chemisorption energy which up to now has been written as a sum of contributions from each perturbed atom (eqs. (110) and (111)), it is easier to compute directly the variation of local

correlation energies instead of computing the self-energies. Using a local approximation and a second order perturbation theory in the band limit⁽³⁰⁾⁽⁴⁰⁾, one can show that the contribution of electronic correlations on atom i to the total energy is given by :

$$E_{\text{cor}}^i = - \frac{L_i(L_i-1)}{2} U_i^2 \int_{E_F}^{\infty} dE_1 \int_{E_F}^{\infty} dE_2 \int_{-\infty}^{E_F} dE_3 \int_{-\infty}^{E_F} dE_4 \frac{n_i(E_1)n_i(E_2)n_i(E_3)n_i(E_4)}{E_1 + E_2 - E_3 - E_4} \quad (113)$$

where L_i , U_i , $n_i(E)$ are respectively the number of spin-orbitals, the effective Coulomb integral (U on the adatom, U_s in the substrate) and the local density of states at site i . Note that this correlation term accounts for the variation of Coulomb energy due to instantaneous fluctuations of the total number of electrons on each site. This clearly cancels in a free atom. An order of magnitude of this quantity is given by⁽⁴¹⁾ :

$$E_{\text{cor}}^i \approx - \frac{L_i(L_i-1)}{2} \frac{U_i^2}{W_i} \left[\frac{N_i}{L_i} \right]^2 \left[1 - \frac{N_i}{L_i} \right]^2 \quad (114)$$

where N_i and W_i are respectively the number of electrons and an effective band width at site i .

Similarly to the band contribution (eq. (109)), one has, with obvious notations :

$$\Delta E_{\text{cor}} = E_{\text{cor}}^a + \sum_i \Delta E_{\text{cor}}^i \quad (115)$$

where E_{cor}^a is negative (eq. (113)) and ΔE_{cor}^i is positive since the presence of the adsorbate increases the effective band width and therefore decreases E_{cor}^i (eq. (114)). As a consequence the sign of the correlation contribution may depend on the adsorbate or on the substrate.

This model can be used to study chemisorption on flat or stepped surfaces and also the adsorption of simple molecules. In the next section we will review the results obtained in all these cases.

4 - 2. Adsorption of simple elements on bcc transition metal surfaces.

We will now present the results obtained with the improved model for the adsorption of simple elements on bcc surfaces.

4 - 2. 1. Low-index faces⁽³³⁾⁽³⁴⁾⁽³⁵⁾.

Let us consider a semi-infinite bcc crystal limited by a (110) or (100) surface. We assume this surface to be the perfect termination of the bulk metal (i. e. there is neither perpendicular relaxation nor reconstruction). The number of d electrons of the substrate will be varied between 3 and 7 electrons per atom since the bcc transition metals correspond to these band fillings. The adsorption sites are expected to be on high symmetry positions (see Fig. 12). Calculations have been performed for various adsorbates : transition atoms⁽³³⁾, N, O, F⁽³⁴⁾ and H⁽³⁵⁾ which interact with the metal d orbitals through their d (transition atoms), p (N, O, F) and s (H) valence orbitals.

The semi-infinite crystal hopping integrals ($dd\lambda$, $\lambda = \sigma, \pi, \delta$) and their variation with distance are obtained from interpolation schemes⁽⁴²⁾. Although they vary slightly between $N_d = 3$ and 7 d electrons per atom, we can with a good approximation neglect this variation. These hopping parameters are also used for adsorbate-substrate interactions in the case of transition adatoms. Adsorbate-substrate hopping integrals depend on two parameters $pd\sigma$, $pd\pi$ with $pd\pi \approx -pd\sigma/2$ for N, O, F and only one, $sd\sigma$, for H adsorption. They can be determined either directly from their definition⁽⁴³⁾ (similar to eq. (49)) or from an interpolation scheme on the band structure of the corresponding covalent compound when it exists. The tight-binding parameters being fixed, the parameters of the Born-Mayer potential are fitted to reproduce known experimental quantities. In the case of transition adatoms they are determined from the values of cohesive energy and bulk modulus and

they must satisfy the bulk equilibrium equation. In the case of O and H, they have been chosen to give reasonable values of the binding energy, bond length and stretch vibration frequency of O and H on W(110). We assume that these parameters do not vary rapidly from an element to its neighbour in the periodic table, thus we take the same values for N and F as for oxygen.

The last parameters of the model are the Coulomb integrals. In atoms, the Coulomb repulsion U is given by the difference between the ionization I and affinity energy A (see eq. (2)). Usually A is much smaller than I and U is therefore of the order of several eV. In transition metals the value of U is strongly reduced from the free atom value by screening. It has been shown that $U_s \sim 1 - 3$ eV⁽⁴¹⁾⁽⁴⁴⁾⁽⁴⁵⁾. For a chemisorbed atom, the Coulomb integral is also lowered by screening which far from the surface of the metal is due to the image potential (see eq. (8)). Therefore a precise determination of the Coulomb integral is extremely difficult for this parameter depends on the distance from the adsorbate to the surface. Since our goal in this work is to determine trends we have made the simplifying assumption of taking U as a constant around the equilibrium position. For N, O and F we have taken $U_a = 2U_s$, this relation is roughly true in the atomic state and therefore we have assumed that the Coulomb interactions are screened to the same extent in the metal and the adsorbate. For H we have chosen $U = 2$ eV⁽³⁵⁾. These values of the Coulomb integrals may seem somewhat small but it is known that the second order perturbation theory tends to exaggerate correlation effects⁽⁴⁰⁾.

4 - 2. 1. a) Adsorption of transition adatoms.

The bond lengths and binding energies of a transition adatom on a substrate of the same chemical species are shown in Figs. 13 and 14 for the different adsorption sites shown in Fig. 12. One sees that the bond length increases with the coordination number. It has a minimum near the middle of the series for a given site, similarly to the variation of the atomic volume

along the transition series. In addition, taking into account the electronic correlation contribution without changing band and repulsion parameters increases the bond length since in this case the main term in ΔE_{cor} is $E_{\text{cor}}^{\text{a}}$ which is negative and increases in absolute value with distance at least around the equilibrium position. On the other hand, binding energies increase with the coordination number and the most stable site corresponds to the most coordinated site available on the surface : centered site on (100) and almost perfect ternary site on (110). They reach a maximum for an almost half-filled band similarly to the cohesive energy. Note that we have neglected the variation of exchange energy which should be introduced since the free atom is magnetic and usually the adsorbed atom is not. It would produce a cusp in the middle of the series which corresponds to the special stability of the half filled d atomic shells, due to a maximum of their exchange interaction. As in the case of cohesive energy ⁽⁴¹⁾ this cusp should be especially marked in the 3d metals where these effects are important. The anisotropy between the (100) and (110) faces is small and is even reduced when correlation effects are taken into account (with $U = 1.2$ eV ⁽⁴⁴⁾⁽⁴⁵⁾). Notice that the correlation contribution stabilizes the adatom since $|E_{\text{cor}}^{\text{a}}|$ prevails.

We have also performed binding energy calculations of 5d adatoms on W surfaces since experimental values of binding energies and surface diffusion activation energies on this substrate are available from FIM experiments ⁽⁷⁾⁽⁹⁾. Results are given in Figs. 15 and 16. Experimental values of $|E_{\text{B}}|$ are rather dispersed and thus not conclusive about the anisotropy. However the order of magnitude of $|E_{\text{B}}|$ is in agreement with our calculations. The easiest diffusion paths on (110) and (100) surfaces, and the corresponding diffusion activation energies Q (extrapolated at 0 K) are given in Fig. 16 and compare well with experimental data. In particular one sees that $|E_{\text{B}}|$ and Q have the same behaviour when the adatom scans a transition series.

4 - 2. 1. b) Adsorption of N, O, F and H.

Let us first neglect the correlation energy term. The variation of the bond lengths of N, O, F and H on different sites of bcc (110) and (100) faces is given in Fig. 17 as a function of the substrate band filling. They increase with the coordination number and with the number of d electrons of the substrate at least when $N_{\text{s}} \geq 5$. The corresponding binding energies are given in Fig. 18. The most stable site is the most coordinated site available on the surface save for H where one obtains, for example on the (100) face, an inversion of stability between the bridge and centered sites for $N_{\text{s}} \approx 5$. This inversion of stability seems to occur between Ta(100) and W(100) according to surface core level shift data ⁽⁴⁶⁾. On the other hand, since the adatom-substrate coupling is rather strong and as expected from 4. 1. 2. b), we find that the binding energy of N, O, F and H decreases with the filling of the substrate d band at least for $N_{\text{s}} \geq 4$ and, for a given substrate, when going from N to O and F due to the filling of the antibonding state of the "surface molecule".

If we now take into account the contribution to the binding energy due to electronic correlations, we find that it changes sign along the transition series for N, O and F and decreases $|E_{\text{B}}|$ for H (see Fig. 19). This can be understood easily since $E_{\text{cor}}^{\text{a}}$ is proportional to the number of pairs of spin orbitals in the adatom valence shell which is reduced to 1 in the case of H so that the variation of the correlation energy of nearest neighbours prevails.

Surface diffusion activation energies are shown in Fig. 20a for N, O, F. They decrease with the substrate band filling and are much larger on the (100) than on the (110) close-packed face. Similar results are obtained for H (Fig. 20b). Therefore, the metals at the end of the d series are those for which chemical species, at least N, O, F and H, diffuse easily. Finally our

results are in good agreement with the experimental data for O and H on W(110) (0.58 eV for O ⁽⁴⁷⁾ and 0.21 eV for H ⁽⁴⁸⁾).

4 - 2. 2. Stepped surfaces ⁽⁴⁹⁾⁽⁵⁰⁾⁽⁵¹⁾

Our model is simple enough to be applied to the adsorption on stepped surfaces. Since, in this case the symmetry is rather low, we cannot limit ourselves to symmetrical sites. Therefore the adatom binding energy $E_B(x, y, z)$ is minimized with respect to the coordinate z (Oz perpendicular to the terraces) for given values of x and y . The minimization is repeated after a small translation of the adatom until a unit cell of the surface is scanned. From these results, we draw a contour map of the binding energy from which we can deduce all the interesting physical quantities : most stable adsorption sites and their energy, diffusion energies along any direction.

Practical calculations have been made on a stepped $[m(110) \times (011)]$ bcc transition metal surface shown schematically in Fig. 21 for the adsorption of transition atoms, O and H. A typical binding energy contour map is shown in Fig. 22 for a W adatom on W. The labelling of remarkable sites is given in Fig. 23a (the U and L indices respectively correspond to upper and lower terrace sites). The most stable adsorption site is D_S for transition adatoms and oxygen and T_U for H although, in this last case, the difference with D_S is small. Possible diffusion paths are shown in Fig. 23 a. In all cases, the diffusion parallel to the ledge is fairly insensitive to the presence of the step even for an adatom diffusing in the ledge. The diffusion across the step, as evidenced by the profiles of the potential energy of the adatom along this direction is strongly perturbed in the case of transition adatoms (Fig. 23 b). This perturbation gets smaller and smaller when going to O and H. Let us point out that a transition adatom moving on the upper terrace is reflected by the outer edge of the step due to the occurrence of an extra barrier height which does not exist for O and H. This effect has been seen in FIM experiments ⁽¹⁰⁾

as stated in the introduction. Moreover the site T_U close to the ledge is slightly more stable than other ternary sites. This type of behaviour has been observed using FIM for a W adatom on the (211) pole of a W tip ⁽¹⁰⁾.

In the case of transition adatoms, calculations have also been performed for the same terrace orientation but for different orientations of the ledge (Figs. 24 a and b). The corresponding potential energy profiles for diffusion across the ledge are drawn in Figs. 24 c and d. Although this calculation confirms the trends discussed above, one sees that the potential energy profile varies significantly with the roughness of the ledge.

5 - BRIEF SUMMARY OF OTHER METHODS.

5 - 1. Effective medium theory ⁽⁶²⁻⁶⁴⁾

Due to its underlying assumption (the starting point being the jellium model), this method is particularly suitable to the study of adsorption on simple and noble metals. However, it has also been used for transition substrates, the effect of d electrons, treated as a perturbation, being superimposed to the effective medium treatment.

The basic idea of the effective medium theory is to replace the metal by a simple effective medium. The simplest medium is obviously a jellium with a density $\bar{\rho}_0 = \rho_0(\vec{r}_a)$, $\rho_0(\vec{r}_a)$ being the substrate electron density at the point where the adatom is located. As a first approximation the adsorption energy can be taken as the difference in energy between the combined adatom-jellium system and a separated atom and jellium :

$$E_B^0(\vec{r}_a) = \Delta E^{\text{hom}}(\bar{\rho}_0) \quad (116)$$

In this scheme, the host is characterised by $\bar{\rho}_0$ only and the quantity $\Delta E^{\text{hom}}(\bar{\rho}_0)$ can then be calculated once for all for each atom or molecule ⁽⁶⁵⁾. The first order correction to this term, due to the inhomogeneity of the electron gas in the vicinity of the surface, can be written :

$$\Delta E_B^1(\vec{r}_a) = \int_a \phi_0(\vec{r}) \Delta \rho_a(\vec{r}) d^3r \quad (117)$$

the integration is performed inside a region a , centred on the adatom, outside which the perturbation due to the adatom can be considered as negligible. $\phi_0(\vec{r})$ is the electrostatic potential of the host and $\Delta\rho_a(\vec{r})$ is the adatom induced perturbation of the charge density in the homogeneous electron gas to which a suitable constant is added so that the volume a is rigorously neutral.

Finally a third term should be added which can be written :

$$\Delta E_{cov} = \delta \int_0^{E_F} \Delta n(E) E dE \quad (118)$$

this term is the difference in the sum of the one-electron energies of the adatom induced states (density of states $\Delta n(E)$) between the effective medium and the real host.

In the case of transition metals ΔE_{cov} contains the effect of the host d electrons which is treated to second order in perturbation. This is to our opinion, the weak point of this theory since, for all transition metal except perhaps at the end of the series, d electrons give the main contribution to the chemisorption.

For more details about this method the reader is referred to B. Lundqvist in this college.

5 - 2. Quantum chemistry method⁽⁶⁶⁾⁽⁶⁷⁾

The quantum chemistry methods most usually replace the semi infinite substrate by a limited number of atoms, the cluster having the same symmetries as the adsorption site. The chemisorption system is studied either by ab initio (X α , Hartree-Fock...) or semi-empirical methods (Hückel, Extended Hückel...). The obvious question that arises is whether the small aggregates mimic correctly the metal. This is questionable when the number of atoms is small since a discrete energy spectrum may be a poor approximation of the true density of states of the metal. Moreover, it is not obvious that the small cluster should have the same electronic configuration as the bulk metal.

Here we will restrict ourselves to a short discussion of the methods that are closest to those developed in the previous section i. e. the Hückel and extended Hückel methods which both rely on an expansion of the electron wave functions as linear combination of atomic orbitals. In the Hückel method the overlap between neighbouring atomic orbitals is neglected so that this method is completely similar to the tight-binding approximation of physicists. In extended Hückel theory this overlap is not neglected and the energy levels are the solutions of the equation :

$$\text{Det } | H_{ij} - ES_{ij} | = 0 \quad (119)$$

with $H_{ij} = \langle i | H | j \rangle$ and $S_{ij} = \langle i | j \rangle$

(For simplicity we have assumed that there is only one orbital $| i \rangle$ per site). The overlap integral are calculated from their definition using atomic orbitals, for instance of the Slater-type. The intraatomic matrix elements H_{ii} of H is the energy of orbital $| i \rangle$ (referred to the vacuum level), they can vary with the charge of atom i and its neighbours (Madelung energy). Finally one finds in the literature many expressions for the interatomic matrix elements H_{ij} as a function of S_{ij} and H_{ii} , the most popular one being the Wolfsberg-Helmholz formula⁽⁶⁸⁾

$$H_{ij} = K S_{ij} (H_{ii} + H_{jj})/2 \quad (120)$$

This method has been widely used by R. Hoffmann⁽⁶⁹⁾.

6 - ADSORPTION OF HOMONUCLEAR DIATOMIC MOLECULES ON METALS

6 - 1. Outline of the problem

As we have seen previously a considerable amount of work has been done in the case of single atom chemisorption from which some general trends have been put forward, for instance concerning the variation of binding energies with the nature of adsorbates and substrates.

On the contrary the present knowledge of the chemisorption of molecules has not reached up to now a similar level. In particular it is of

primary importance to know whether a molecule approaching a surface will dissociate or not.

Quantitatively, when a diatomic molecule X_2 approaches a metal surface, it may encounter three types of potential wells corresponding to a physisorbed state (far from the surface), then when its orbitals begin to mix with the metal ones a molecular chemisorbed state may exist, the last well corresponding to dissociative chemisorption. If we disregard the physisorbed state, which is out of the scope of this study, the potential energy diagram may be of the Lennard-Jones type ⁽⁶⁰⁾ (see Fig. 25) with the existence or not of an activation barrier ΔE^{\ddagger} for dissociation. From this diagram an obvious necessary condition for dissociative chemisorption is the occurrence of an energy gain when going from the molecular chemisorbed state to the dissociated one

$$2 | E_{\text{ads}}(X) | > E_{\text{diss}}(X_2) + | E_{\text{ads}}(X_2) | \quad (121)$$

where $E_{\text{ads}}(X)$ is the atomic adsorption energy (< 0) of atom X , $E_{\text{diss}}(X_2)$ and $E_{\text{ads}}(X_2)$ are respectively the dissociation energy (> 0) of the free molecule and its molecular chemisorption energy (< 0). For $X = \text{N}, \text{O}, \text{F}, \text{H}$, $| E_{\text{ads}}(X) |$ being a decreasing function when going across a transition series, this inequality may not be satisfied above some critical band filling. This qualitatively explains that the dissociative chemisorption of N_2 and NO , for instance, occurs for metals on the left of transition series whereas on the right one observes a tendency to molecular adsorption ⁽¹²⁾ (Table II).

However the question of whether or not a molecule dissociates at the surface is a very complicated problem. The answer will depend on the dynamical motion of the molecule impinging on the surface and on the molecule-substrate energy transfers. Any attempt to treat this problem should start from the calculation of potential energy surfaces. The potential energy is the total

ground state energy of the chemisorption system minus that of the constituents calculated as a function of the coordinates of the involved atoms. The determination of these potential energy surfaces can be investigated by different techniques derived either from quantum chemistry or from solid state physics theories. In the former approach, one treats the adsorbed atoms and a small number of neighbouring solid atoms as a surface molecule while the latter starts from a semi-infinite crystal on which the effect of the adatoms is superimposed. Among the quantum chemistry methods one of the most popular for this type of problems is the LEPS (London-Eyring-Polanyi-Sato) approach which is basically a valence bond treatment derived from the determination of the potential energy of a system of four one electron atoms ⁽⁶⁰⁾. The LEPS potential has the advantage of being easy to evaluate numerically for any arrangement of atoms and can therefore be used as input in dynamical calculations ⁽⁶¹⁾. However in this approximation the electrons are assumed to be strongly localised which is questionable for chemisorption on metal surfaces. On the other hand the delocalisation of the valence electrons in the metal has been taken into account for strongly delocalised electrons only (i. e. for simple and noble metals), the most appropriate method being the Local Density Functional (LDF) within the effective medium theory ⁽⁶²⁾. When the electrons of the metal are more localised (valence d electrons of transition metals) the tight-binding theory has been well effective to explain the general trends seen in atomic adsorption. This method can be applied to compute potential energy surfaces for diatomic homonuclear molecules interacting with a transition metal surface ⁽⁶³⁾. It takes into account the delocalised character of the electrons, and is of rather simple use to calculate potential energy surfaces for molecules in many geometrical configurations. This approach includes correctly the existence of a continuous spectrum of energy levels in the solid but it certainly gives a rather poor

description of the free molecule. For most realistic systems an adequate description of the molecule-surface interaction should be intermediate between the localised picture (LEPS) and the delocalised one.

6 - 2. Adiabatic potential energy surfaces for diatomic molecules on transition metal surfaces ⁽⁶³⁾.

Let us consider a frozen substrate. In this case, the adiabatic potential energy surfaces for a diatomic molecule are hypersurfaces in the 6-dimensional space spanned by the three coordinates of both adsorbates but, if we reduce the number of degrees of freedom of the molecule by assigning a given geometry of approach, the dimension of these hypersurfaces is lowered.

In the following, we apply the models previously developed for the atomic adsorption to the case of the chemisorption of diatomic homonuclear molecules on simple bcc transition metal surfaces neglecting the electronic correlation term. We consider a X_2 molecule impinging normally on the surface with its axis parallel to it. Moreover it is assigned to stay in a given plane, and the projection of its center of gravity on the surface is a high symmetry point so that the two X atoms are equivalent. Within these restrictions the potential energy contour maps are only function of two coordinates (the distance to the surface and the molecule interatomic distance).

In a first approach, all local densities of states are assumed to have a rectangular shape with a width fitted to the exact second moment. In addition the perturbation of the substrate is taken into account and similarly to the atomic case, charge neutrality of each involved atom is assumed. Practical calculations have been made for a molecule with an half filled p valence shell interacting with a (100) surface of a bcc transition metal with a half filled d band. We have taken $p_{XX}/q_{XX} = p_{XM}/q_{XM} = 3$, $q_{XX} d_\infty = q_{XM} R_1 = 3$ where d_∞ is the bond length of the free molecule and R_1 the bond length of a

single X adsorbed atom, the indices XX and XM refer respectively to the X-X and X-metal bond.

The remaining parameters A_{XX} , A_{XM} , β_{XX} , β_{XM} i. e. respectively the prefactors of the Born-Mayer potentials and the hopping integrals between two X atoms and between a X atom and a metal atom M are deduced from the values of R_1 , d_∞ , $E_{ads}(X)$ and $E_{diss}(X_2)$. The considered geometries are given in the insets of Fig 26 and the corresponding potential energy contour maps are drawn in Figs. 26 (a, b, d, e). We have also plotted (Figs. 26 c and f) the minimum value $E_B^{min}(X_2)$ with respect to the molecular interatomic distance as a function of the distance to the surface for four values of $E_{diss}(X_2)$, the other parameters being fixed. In Figs. 26 a and b the potential energy contour maps exhibit first a single well corresponding to a dissociative chemisorption, then a second well appears farther from the surface corresponding to the molecular chemisorption which, for large values of $E_{diss}(X_2)$, becomes the most stable adsorption site. On Fig. 26 c, one sees that the energy of the saddle point is larger than the energy of the free molecule for $E_{diss}(X_2) = 9$ and 12 eV. In this case the molecule needs an activation energy ΔE^* to dissociate. In Figs. 26 d and e the potential energy contour lines present two wells at similar distances from the surface corresponding to atomic and molecular chemisorption (the molecular well being deeper when $E_{diss}(X_2)$ is large). This case occurs when the two atoms separating to reach atomic adsorption sites pass by a saddle point for atomic adsorption. The plots $E_B^{min}(X_2)$ as a function of the distance to the surface are shown in Fig. 26 f. This computation shows clearly the influence of $E_{diss}(X_2)/|E_{ads}(X)|$. In particular, in a given range of values of this ratio (1.3 - 2), the existence of both atomic and molecular adsorption wells is expected.

From the above results we observe that when a molecular well exists the interatomic distance of the molecule varies only slightly from the equilibrium value of the free state. This suggests to set up a more simplified model in which we compare the adsorption energy of a rigid molecule X_2 with the one of two isolated X adatoms. Furthermore if we neglect the substrate contribution to the binding energy and assume that all X-substrate bonds are equivalent the relevant energies can be expressed analytically as a function of $E_{diss}/|E_{ads}|$ and geometrical parameters. From these expressions we can derive many of the trends put forward in the preceding calculations and thus clarify the respective roles played by energetic and geometrical factors. In this model the binding energy of the molecule corresponding to interatomic distance d is approximated by

$$E_B^{\infty}(X_2) = A_{XX} e^{-3q_{XX}\left[\frac{d}{d_{\infty}} - 1\right]} - 2B\beta_{XX} e^{-q_{XX}\left[\frac{d}{d_{\infty}} - 1\right]} \quad (122)$$

in which B is a function of N_X only. N_X between the number of valence electrons of an X atom. The dissociation energy, taking the equilibrium condition into account ($3A_{XX} = 2B\beta_{XX}$), is given by

$$E_{diss} = - \left[E_B^{\infty}(X_2) \right]_{d=d_{\infty}} = \frac{4}{3} B\beta_{XX} = 2A_{XX} \quad (123)$$

In the same way the binding energy of an X isolated adatom with coordination number Z and bond length R is

$$E_B(X) = ZA_{XM} e^{-3q_{XM}\left[\frac{R}{R_1} - 1\right]} - B \sqrt{Z}\beta_{XM} e^{-q_{XM}\left[\frac{R}{R_1} - 1\right]} \quad (124)$$

where B is the same function of N_X as above and R_1 is the equilibrium bond length. Taking the equilibrium condition into account ($3ZA_{XM} = B \sqrt{Z}\beta_{XM}$), the adsorption energy is :

$$E_{ads} = \left[E_B(X) \right]_{R=R_1} = - \frac{2}{3} B \sqrt{Z}\beta_{XM} = - 2ZA_{XM} \quad (125)$$

Finally the energy of a flat rigid molecule ($d = d_{\infty}$) interacting with the substrate is :

$$E_B(X_2) = 2Z'A_{XM} e^{-3q_{XM}\left[\frac{R'}{R_1} - 1\right]} + A_{XX} - 2B \sqrt{Z}\beta_{XM} e^{-2q_{XM}\left[\frac{R'}{R_1} - 1\right]} + \beta_{XX}^2 \quad (126)$$

where Z' and R' are respectively the number of substrate neighbours of each atom X and the corresponding bond length. At the equilibrium position ($R' = R_1$) we have

$$e^{-2q_{XM}\left[\frac{R'}{R_1} - 1\right]} = \frac{1}{8} \frac{Z'}{Z} \left[\frac{E_{diss}}{E_{ads}} \right]^2 (-1 + S) \quad (127)$$

$$\text{with } S = \sqrt{1 + 64 \frac{Z'}{Z} \left[\frac{E_{ads}}{E_{diss}} \right]^4}$$

from which we deduce

$$E_B^{R_1}(X_2) = \left[E_B(X_2) \right]_{R'=R_1} = \frac{E_{diss}}{2} \left\{ 1 + \frac{1}{8\sqrt{2}} \left(\frac{Z'}{Z} \right)^{1/2} \left[\frac{E_{diss}}{E_{ads}} \right]^2 (-1 + S)^{3/2} - \frac{3}{\sqrt{2}} (1+S)^{1/2} \right\} \quad (128)$$

In Fig. 27, we have plotted $E_B^{R_1}(X_2)/E_{ads}$ as a function of $|E_{diss}/E_{ads}|$: we see that $|E_B^{R_1}(X_2)|$ increases with Z' for given values of Z , E_{diss} and E_{ads} . On the other hand, the energy gain when adsorbing the molecule, $|E_B^{R_1}(X_2) + E_{diss}|$, decreases continuously towards zero when E_{diss} increases. The molecular adsorption is energetically favorable when $E_B^{R_1}(X_2) \leq 2 E_{ads}$ i. e. when $|E_{diss}/E_{ads}| \geq 1.7$ for $Z'/Z = 1/2$ and $|E_{diss}/E_{ads}| \geq 1.9$ for $Z'/Z = 1/5$, thus the transition between atomic and molecular adsorptions is rather independent of the geometry.

Let us now consider the geometries of approach for which the distance to the surface of the molecular adsorption well is much larger than the atomic one. In these cases, we have seen that the saddle point between the two wells may be above the energy of the free molecule giving rise to an activation energy for dissociation. This occurs for the particular geometry of Fig. 26 b when E_{diss} is larger than a critical value. In the framework of this

simplified model we have to find the crossing point between the atomic and molecular potential curves and examine if the corresponding energy is larger or smaller than $-E_{\text{diss}}$. The critical value is thus given by

$$2 \left[E_B(X) \right]_{z=z_c} = -E_{\text{diss}} \quad (129 \text{ a})$$

$$\left[E_B(X_2) \right]_{z=z_c} = -E_{\text{diss}} \quad (129 \text{ b})$$

In the physically interesting situation the crossing point is rather far from the z position of the bottom of the atomic well, i. e. in the attractive part, and the repulsive contribution can be neglected. Under this condition eqs. (124), (125) and (129 a) give :

$$\frac{-q_{XM} \left[\frac{R(z_c)}{R_1} - 1 \right]}{e} = -\frac{E_{\text{diss}}}{3E_{\text{ads}}} \quad (130)$$

similarly eqs. (123), (126) and (129 b) give

$$\frac{Z'}{Z} Y_m^4 - 3 \frac{E_{\text{diss}}}{E_{\text{ads}}} Y_m - 9 = 0 \quad (131)$$

$$\text{with } Y_m = e^{-q_{XM} \left[\frac{R(z_c)}{R_1} - 1 \right]}$$

Eliminating z_c between eqs. (130) and (131) we get an implicit equation in $|E_{\text{diss}}/E_{\text{ads}}|$. Its solution gives the critical value of $|E_{\text{diss}}/E_{\text{ads}}|$ above which an activation barrier exists. This can be done quite easily on a computer in order to obtain the critical value η_c of $|E_{\text{diss}}/E_{\text{ads}}|$ as a function of d_∞ for various values of Z and Z' . The only physically interesting solution corresponding to dissociative activated adsorption ($\eta_c < 2$) occurs in the case of geometry of Fig. 26 b. One finds ⁽⁶³⁾ that an increase of d_∞ (i. e. a decrease of the lateral distance between the atomic and molecular wells) leads to slightly larger value of η_c whereas changing the geometry of approach (i. e. Z'/Z) is quite crucial.

As in the atomic adsorption case, we can perform more realistic calculations using local densities of states obtained from a continued

fraction expansion of the local Green function on the atom i with three exact coefficients a_1^i , b_1^i , a_2^i . We have done such computations for an O_2 molecule arriving on the (110) and (100) faces of a transition metal with a half filled d band. The parameter describing the interaction between an oxygen atom and a substrate atom are the same as in section 4. The potential energy curve of the free O_2 molecule is assumed to be Morse-like ($p_{XX}/q_{XX} = 2$), and we assume $|pp\sigma|/|pp\pi| = 2$; the remaining parameters for the O-O interaction : $pp\sigma$, q_{XX} and Λ_{XX} are determined to fit $E_{\text{diss}}(O_2)$, d_∞ and the stretch vibration frequency.

Results are shown in Figs. 28 and 29 with the corresponding geometry of approach. One sees in Fig. 28 that on the (100) face the molecule dissociates. However its final energy is not twice the atomic adsorption energy since there is a repulsive indirect (via the two substrate atoms labelled 1 in Fig. 28) interaction energy between the two atoms.

The case exhibited in Fig. 29 is not so clearcut since the distance between the two atoms in the adsorbed state is such that there still exists a sizeable direct interaction between them. Energy calculations are not sufficient to decide whether the molecule is dissociated or not. A more appropriate quantity would be the electron density between atom pairs which is connected to the bond order. This last quantity is quite familiar to quantum chemists. It can also be easily calculated using the Green function technique since it is connected to the interatomic Green function. For example, between two atoms i and j with only one atomic orbital, it can be written :

$$P_{ij} = -\frac{1}{2\pi} \int_{-\infty}^{E_F} \text{Im} \left[G_{ij}(E + i0^+) + G_{ji}(E + i0^+) \right] dE \quad (132)$$

Qualitatively one expects that making bonds between the molecule and the substrate usually weakens the intramolecular bond, this is indeed found using simple models ⁽⁶³⁾.

7 - CONCLUSIONS

In summary we have shown that, in spite of its incompleteness, the theoretical description of chemisorption of simple elements on metals can provide an understanding of the main trends observed experimentally. In particular for substrates at the end of the transition series one expects moderate binding energies, small activation energies for surface diffusion and possible existence of both molecular and dissociative chemisorption. These three factors are clearly favourable for surface chemical reactions and this should be one of the reasons why the best catalysts are found at the end of the transition series.

However there is still a long way before we understand fully the dynamics of adsorption and surface reactions since this involves the complete treatment of the energy transfers via phonons or electron hole pairs from the adatom to the substrate or vice-versa. The comparison between molecular dynamics simulations and molecular beam experiments should provide useful information on this problem.

APPENDIX 1

Let us consider a semi-infinite linear chain with one orbital per site, $-\beta$ ($\beta > 0$) being the hopping integral between nearest neighbours.



Let us calculate the local density of states on the first atom using the Green function technique : in the basis of atomic orbitals.

$$G = (z - H)^{-1} = \begin{vmatrix} z & \beta & & \\ \beta & z & \beta & \\ & \beta & z & \beta \\ & & \ddots & \ddots & \ddots \end{vmatrix}^{-1}$$

in which energies are referred to the atomic level

$$G_{11} = \frac{D_{n-1}}{D_n} = \frac{D_{n-1}}{zD_{n-1} - \beta^2 D_{n-2}} = \frac{1}{z - \beta^2 \frac{D_{n-2}}{D_{n-1}}}$$

D_{n-p} being the determinant obtained by suppressing the first p lines and columns.

Since the chain is semi-infinite $\frac{D_{n-2}}{D_{n-1}} = G_{11}$

Thus

$$G_{11} = \frac{1}{z - \beta^2 G_{11}}$$

and

$$G_{11} = \frac{z + \eta \sqrt{z^2 - 4\beta^2}}{2\beta^2} \quad \begin{matrix} Z = E + i\epsilon \\ \eta = \pm 1 \end{matrix}$$

G_{11} has an imaginary part when $-2\beta < E < 2\beta$. Consequently the bandwidth $W = 4\beta$ and

$$G_{11} = \frac{z + \eta \sqrt{z^2 - \frac{W^2}{4}}}{W^2/8}$$

The value of η outside the band should be such that G_{11} behaves like $1/z$ when E tends to infinity. Thus :

$$\eta = +1 \quad \text{when } E < -2\beta$$

$$\eta = -1 \quad \text{when } E > 2\beta$$

Inside the band, $\text{Im } G_{11}$ should be negative to get a positive density of states

$$\eta \sqrt{z^2 - \frac{W^2}{4}} = -1 \sqrt{\frac{W^2}{4} - E^2}$$

APPENDIX 2

Let us consider an unperturbed hamiltonian H_0 and a perturbed one $H = H_0 + V$ and calculate the variation $\Delta n(E)$ of the density of states due to the perturbation.

One has :

$$(E - H + i\epsilon) \frac{1}{E - H_0 \pm i\epsilon} = 1 - VG_0^\pm(E)$$

$G_0^\pm = (E - H_0 \pm i\epsilon)^{-1}$ is the unperturbed Green function. We thus get :

$$\text{Det}(1 - VG_0^\pm(E)) = \pi \frac{E - E_j \pm i\epsilon}{\prod_j E - E_j^0 \pm i\epsilon}$$

E_j and E_j^0 being respectively the eigenvalues of H and H_0

$$\frac{d}{dE} \text{Log Det}(1 - VG_0^\pm(E)) = \sum_j \frac{1}{E - E_j \pm i\epsilon} - \sum_j \frac{1}{E - E_j^0 \pm i\epsilon}$$

Let us take the imaginary part of this expression :

$$\text{Im} \frac{d}{dE} \text{Log Det}(1 - VG_0^\pm(E)) = \mp \pi \left\{ \sum_j \delta(E - E_j) - \sum_j \delta(E - E_j^0) \right\}$$

$$\Delta n(E) = \mp \frac{1}{\pi} \text{Im} \frac{d}{dE} \text{Log Det}(1 - VG_0^\pm(E))$$

APPENDIX 3

Let us show that in the Hartree-Fock approximation :

$$\int_{\sigma}^F (E-E_F) \Delta N(E) dE = \frac{1}{2\pi i} \int_C (z-E_F) \left(1 - \frac{\partial S}{\partial z}\right) c_{aa}^{\sigma\sigma}(z) dz$$

where C is the contour consisting of the real axis and a semi-circle at infinity in the upper half plane and $c_{aa}^{\sigma\sigma}(z)$ is the causal Green function. The integral on the semi-circle vanishes and therefore the second member of the preceding equation can be written :

$$\lim_{\epsilon \rightarrow 0} \frac{1}{2\pi i} \int_{\sigma} \left\{ \int_{-\infty}^{E_F} (E-E_F) \left(1 - \frac{\partial S(E-i\epsilon)}{\partial E}\right) c_{aa}^{\sigma\sigma-}(E-i\epsilon) dE \right. \\ \left. + \int_{E_F}^{+\infty} (E-E_F) \left(1 - \frac{\partial S(E+i\epsilon)}{\partial E}\right) c_{aa}^{\sigma\sigma+}(E+i\epsilon) dE \right\}$$

$$\lim_{\epsilon \rightarrow 0} \frac{1}{2\pi i} \int_{\sigma} \left\{ \int_{-\infty}^{E_F} (E-E_F) \left(1 - \frac{\partial S(E-i\epsilon)}{\partial E}\right) c_{aa}^{\sigma\sigma-}(E-i\epsilon) dE \right. \\ \left. - \int_{-\infty}^{E_F} (E-E_F) \left(1 - \frac{\partial S(E+i\epsilon)}{\partial E}\right) c_{aa}^{\sigma\sigma+}(E+i\epsilon) dE \right. \\ \left. + \int_{E_F}^{+\infty} (E-E_F) \left(1 - \frac{\partial S(E+i\epsilon)}{\partial E}\right) c_{aa}^{\sigma\sigma+}(E+i\epsilon) dE \right\}$$

The third integral can be transformed into a contour integra. on C which vanishes since the poles are below the real axis. Then using eq. 64 c of the main text valid in the Hartree-Fock approximation, we find immediately the equation to be proved.

	Ni (111) Z = 3	Ni (100) Z = 4
d _{O-Ni}	1.88 Å	1.98 Å
d _{S-Ni}	2.02 Å	2.19 Å
d _{Se-Ni}	2.31 Å	2.35 Å

TABLE I

Experimental variations of the bond lengths of O, S and Se on Ni as a function of the coordination number (from refs. ⁽²⁾ and ⁽³⁾).

Sc	Ti	V	Cr	Mn	Fe	Co	Ni	Cu
Y	Zr	Nb	Mo	Tc	Ru	Rh	Pd	Ag
La	Hf	Ta	W	Re	Os	Ir	Pt	Au

TABLE II

Borderline between dissociative (left hand side) and molecular (right hand side) chemisorption at room temperature : thick line, N_2 : double line, NO from ref. (12).

REFERENCES

- (1) see for example D. A. Woodruff and T. A. Delchar, Modern Techniques of surface science, Cambridge Solid State Sci. Series, Cambridge University Press, Cambridge (1986)
- (2) J. E. Demuth, D. W. Jepsen and P. M. Marcus, Phys. Rev. Lett. 31, 540, (1973), 32, 1182 (1974)
 - M. A. Van Hove and S. Y. Tong, J. Vac. Sci. Technol. 12, 230 (1975)
 - P. M. Marcus, J. E. Demuth and D. W. Jepsen, Surf. Sci. 53, 501 (1975)
 - D. H. Rosenblatt, S. D. Kevan, J. G. Tobin, R. F. Davis, M. G. Mason, D. R. Denley, D. A. Shirley, Y. Huang and S. Y. Tong, Phys. Rev. B 26, 1812 (1982)
- (3) K. A. R. Mitchell, Surf. Sci. , 149, 93 (1985)
- (4) J. Sokolov, F. Jona and P. M. Marcus, Sol. St. Comm. 49, 307 (1984) and references therein
- (5) M. R. Barnes and R. F. Willis, Phys. Rev. Lett. 41, 1729 (1978)
- (6) I. Toyoshima and G. A. Somorjai, Catal. Rev. Sci. Eng. 19, 105 (1979)
- (7) A. Menand and J. Gallot, Rev. Phys. Appl. 9, 323 (1974)
- (8) G. Bolbach, Thesis Paris (1982)
- (9) D. W. Bassett, Surf. Sci. 53, 74 (1975), J. Phys. C : Solid St. Phys. 9, 2491 (1976)
- (10) H. W. Fink and G. Ehrlich, Surf. Sci. 143, 125 (1984)
- (11) J. Cousty, Thesis, Orsay (1980)
- (12) G. Brodén, T. N. Rhodin, C. Brucker, R. Benbow and Z. Hurych, Surf. Sci. 59, 593 (1976)
- (13) J. R. Schrieffer, Proceedings of the International School of Physics, Enrico Fermi, Course LVIII Dynamical Aspects of Surface Physics, Ed. by F. O. Goodman, Ed. Compositori, Bologna (1974)
- (14) P. W. Anderson, Phys. Rev. 124, 41 (1961)
- (15) T. B. Grimley, Proc. Phys. Soc. 90, 751, 92, 776 (1967)
- (16) D. M. News, Phys. Rev., 178, 1123 (1969)
- (17) M. C. Desjonquères, Thesis, Grenoble (1976)
- (18) M. J. Kelly, Surf. Sci. 43, 587 (1974)
- (19) M. C. Desjonquères and F. Cyrot Lackmann, Solid St. Comm. 26, 271 (1978)
- (20) J. Friedel, Phil. Mag. Supp. 3, 446 (1954)

- (21) W. Brenig and K. Schönhammer, *Zeit. Phys.* **267**, 201 (1974)
- (22) B. Bell and A. Madhukar, *Phys. Rev. B* **14**, 4281 (1976)
- (23) K. Schönhammer, *Sol. St. Comm.* **32**, 51 (1977)
- (24) M. Baldo, F. Flores, A. Martín-Rodero, G. Piccitto and R. Pucci, *Surf. Sci.* **128**, 237 (1983)
- (25) M. Baldo, R. Pucci, F. Flores, G. Piccitto, A. Martín-Rodero, *Phys. Rev. B* **28**, 6640 (1983)
- (26) O. Gunnarsson and K. Schönhammer, *Phys. Rev. Lett.* **41**, 1608 (1978)
- (27) B. Kjällerström, D. J. Scalapino and J. R. Schrieffer, *Phys. Rev.* **148**, 665 (1966)
- (28) K. Schönhammer, V. Hartung and W. Brenig, *Zeit. Phys. B* **22**, 143 (1975)
- (29) G. Piccitto, F. Siringo, M. Baldo and R. Pucci, *Surf. Sci.* **167**, 437 (1986)
- (30) G. Tréglia, F. Ducastelle and D. Spanjaard, *J. de Physique* **41**, 281 (1980)
- (31) A. Martín-Rodero, F. Flores, M. Baldo and R. Pucci, *Sol. St. Comm.* **44**, 911 (1982)
- (32) P. Schuck, *Phys. Rev. B* **13**, 5225 (1976)
- (33) M. C. Desjonquères and D. Spanjaard, *J. Phys. C : Solid St. Phys.* **15**, 4007 (1982)
- (34) M. C. Desjonquères and D. Spanjaard, *J. Phys. C : Solid St. Phys.* **16**, 3389 (1983)
- (35) C. Thuault-Cytermann, M. C. Desjonquères and D. Spanjaard, *J. Phys. C : Solid St. Phys.* **16**, 5689 (1983)
- (36) F. Ducastelle, Thesis, Orsay (1972)
- (37) J. C. Slater and G. F. Koster, *Phys. Rev.* **94**, 1498 (1954)
- (38) R. Haydock, V. Heine and M. J. Kelly, *J. Phys. C : Solid St. Phys.* **5**, 2845 (1972)
- (39) J. P. Gaspard and F. Cyrot-Lackmann, *J. Phys. C : Solid St. Phys.* **6**, 3077 (1973)
- (40) G. Tréglia, Thesis, Orsay (1983)
- (41) J. Friedel and C. M. Sayers, *J. de Physique*, **38**, 697, (1977)
- (42) H. Ehrenreich and L. Hodges, *Methods in Comp. Phys.* **8**, 149 (1968)
- (43) Y. Boudeville, J. Rousseau-Violet, F. Cyrot-Lackmann and S. N. Khanna, *J. de Physique* **44**, 433 (1983)
- (44) G. Tréglia, M. C. Desjonquères, F. Ducastelle and D. Spanjaard, *J. Phys. C : Solid St. Phys.* **14**, 4347 (1981)
- (45) G. Tréglia, F. Ducastelle and D. Spanjaard, *J. de Physique* **43**, 341 (1982)

- (46) C. Guillot, C. Thuault, Y. Jugnet, D. Chauveau, R. Hoogewijs, J. Lecante, Tran Minh Duc, G. Tréglia, M. C. Desjonquères and D. Spanjaard, *J. Phys. C : Solid St. Phys.* **15**, 423 (1982)
- C. Guillot, P. Roubin, J. Lecante, M. C. Desjonquères, G. Tréglia, D. Spanjaard and Y. Jugnet, *Phys. Rev. B* **30**, 5487 (1984)
- (47) M. Bowker and D. A. King, *Surf. Sci.*, **94**, 564 (1980)
- (48) R. Di Foggio and R. Gomer, *Phys. Rev. Lett.* **44**, 1258 (1980)
- (49) J. P. Jardín, M. C. Desjonquères and D. Spanjaard, *J. Phys. C : Solid St. Phys.*, **18**, 1767, (1985)
- (50) J. P. Jardín, M. C. Desjonquères and D. Spanjaard, *J. Phys. C : Solid St. Phys.*, **18**, 5759, (1985)
- (51) J. P. Bourdin, J. P. Canachaud, J. P. Jardín, D. Spanjaard and M. C. Desjonquères, *J. Phys. F*, in press (1988)
- (52) M. J. Stott and E. Zaremba, *Phys. Rev. B* **22**, 1564 (1980)
- (53) J. K. Nørskov and N. D. Lang, *Phys. Rev. B* **21**, 2136 (1980)
- (54) J. K. Nørskov, *Phys. Rev. B* **26**, 2875 (1982)
- (55) M. J. Puska, R. M. Nieminen and M. Manninen, *Phys. Rev. B* **24**, 3037 (1981)
- (56) S. P. Mc Glynn, L. G. Vanquickenborne, M. Kinoshita and D. G. Carroll, Introduction to Applied Quantum Chemistry, Holt, Rinehart, Winston inc. ed. (1972)
- (57) P. D. Offenhartz, Atomic and Molecular Orbital Theory, Mc Graw Hill ed. (1970)
- J. A. Pople and D. L. Beveridge, Approximate Molecular Orbital Theory, Mc Graw Hill ed. (1970)
- (58) M. Wolfsberg and L. Helmholz, *J. Chem. Phys.* **20**, 837 (1952)
- (59) J. E. Lennard-Jones, *Trans. Far. Soc.* **28**, 333 (1932)
- (60) H. Eyring, J. Walter and G. E. Kimball, in Quantum Chemistry, John Wiley and sons, Chap. XIII (1967)
- (61) A. Gelb and M. J. Cardillo, *Surf. Sci.* **64**, 197 (1977)
- J. H. Mc Creery and G. Wolken Jr., *J. Chem. Phys.* **67**, 2551 (1977)
- G. F. Tantardini and M. Simonetta, *Chem. Phys. Lett.* **87**, 420 (1982)
- B. C. Khanra and S. K. Saha, *Chem. Phys. Lett.* **95**, 217 (1983)
- (62) J. K. Nørskov, H. Houmoller, P. K. Johansson and B. I. Lundqvist, *Phys. Rev. Lett.* **46**, 257 (1981)
- (63) M. C. Desjonquères, J. P. Jardín and D. Spanjaard, *Surf. Sci.*, in press (1988)

FIGURE CAPTIONS

- Fig. 1 : Experimental binding energies of 5d adatoms on W(111), W(112) and Ir(111) (from Menand and Gallot ⁽⁷⁾).
- Fig. 2 : Variation of the binding energies of N, O, F and H along the transition series (from Toyoshima and Somorjai ⁽⁶⁾ and Bolbach ⁽⁸⁾).
- Fig. 3 : Experimental activation energies for surface diffusion of 5d adatoms on W(110) and (112) (from Bassett ⁽⁹⁾).
- Fig. 4 : Influence of the image potential on the ionization and affinity levels of an adatom.
- Fig. 5 : Electric image of an adatom.
- Fig. 6 : Solution of the Anderson-Grimley-Newns hamiltonian in the weak (a, a') and strong (b, b') coupling limits. (a, b) : intersections of $E - \epsilon_{ao}$ with Λ which define the localized states, (a' b') : corresponding local densities of states on the adsorbate.
- Fig. 7 : The three adsorption sites for an adatom on the (100) surface of a simple cubic lattice.
(a) on top (b) bridge (c) centered.
- Fig. 8 : Local densities of states of an on top adatom on the (100) surface of a simple cubic lattice for various values of the adatom-substrate coupling.
- Fig. 9 : Local density of states of a Mo adatom on Mo compared with the surface density of states. The adatom is assumed to occupy a lattice site.
(a) (110) surface.
(b) (100) surface.

- Fig. 10 : Deformation of the local density of states on the adatom when the substrate band filling (i. e. E_F) varies in the strong coupling limit (ϵ_a^* and ϵ_d are respectively the effective adatom atomic level and the center of the substrate d band).
- Fig. 11 : Schematic variation of the binding energy of an adsorbate with N_a/L_a electrons per orbital as a function of the substrate band filling (i. e. E_F).
- Fig. 12 : Labelling of adsorption sites on the (110) and (100) faces of a bcc metal.
- Fig. 13 : Adatom-substrate bond lengths R_o for several sites on (110) and (100) bcc surfaces for an adatom on a substrate of the same chemical species as a function of the number of d electrons (full curves : $U = 0$, broken curves : $U = 1.2$ eV). R_b is the bulk interatomic distance.
- Fig. 14 : Adatom-substrate binding energy for several sites on (110) and (100) bcc surfaces for an adatom and a substrate of the same chemical species as a function of the number of d electrons (full curves $U = 0$; broken curves $U = 1.2$ eV). The curves labelled T_D refer to the most stable site between B_2 and T.
- Fig. 15 : Calculated binding energies of 5d adatoms on W(110) and (100).
- Fig. 16 : Easiest diffusion paths and their activation energies (extrapolated at 0 K) of 5d adatoms on W (100) and (110) compared with experiments ⁽⁹⁾.

Fig. 17 : Adsorbate-substrate bond lengths for different sites on (110) and (100) bcc surfaces as a function of the number of d electrons of the substrate. For the centered site (C) on (100) two bond-lengths are given : \perp corresponds to the bond perpendicular to the surface, \angle to the bonds with the four metal atoms in the surface plane :

(a) N, O, F adatoms.

(b) H adatoms.

Fig. 18 : Binding energies of N, O, F and H for different sites on (110) and (100) bcc surfaces as a function of the number of d electrons of the substrate.

Fig. 19 : Influence of electronic correlations on the binding energies of N, O, F (a, b) and H (c, d) at their most stable position on (110) and (100) bcc surfaces (full curves $U_a = U_s = 0$, broken curves $U_a = 2U_s = 2.4$ eV for N, O, F and $U_a = 2$ eV, $U_s = 1.2$ eV for H) as a function of the number of d electrons of the substrate.

Fig. 20 (a) : Surface diffusion activation energies at 0 K of N, O, F on (110) and (100) bcc surfaces as a function of the number of d electrons of the substrate.

(b) : Surface diffusion activation energies at 0 K of H on (110) and (100) bcc surfaces as a function of the number of d electrons of the substrate.

Fig. 21 : Schematic geometry of the stepped bcc surface $[m(110) \times (0\bar{1}1)]$.

Fig. 22 : Adatom binding energy contour maps (i. e. contour lines of the surface $E_B^{\min}(x, y)$ where E_B^{\min} is the minimum of $E_B(x, y, z)$ with respect to the coordinate z for a given value of x and y) for W on $W[m(110) \times (0\bar{1}1)]$.

Fig. 23 : a) Labelling of sites and diffusion channels of the $[m(110) \times (0\bar{1}1)]$ bcc stepped surface. The atoms of the upper (lower) terrace are drawn as full (broken) circles.

b) Profile of the potential energy of an adatom diffusing across the step.

(a') W adatom on W.

(b') O on a metal with 5d electrons per atom.

(c') H on a metal with 5d electron per atom.

Fig. 24 : (a, b) Labelling of sites and diffusion channels of the $[m(110) \times (1\bar{1}0)]$ (a) and $[m(110) \times (001)]$ (b) bcc stepped surfaces. The atoms of the upper (lower) terraces are drawn as full (broken) circles.

(a', b') Profile of the potential energy of a W adatom diffusing across a W $[m(110) \times (1\bar{1}0)]$ (a') or $[m(110) \times (001)]$ (b') step.

Fig. 25 : Lennard-Jones potential energy diagram for the chemisorption of a X_2 molecule when molecular and dissociative wells exist. $\Delta E^{\#}$ is the activation barrier for dissociation.

Fig. 26 : Potential energy curves of a homonuclear diatomic molecule X_2 (with $d_{\infty} = 1.2$ Å) for several values of $E_{\text{diss}}(X_2)$ and for the geometries of approach towards a (100) bcc surface shown in the insets. The lattice parameter is $a_0 = 3.16$ Å which corresponds to W. The valence shell of X and the substrate d band are both half filled. a(d), b(e) are respectively the equipotential energy curves for $E_{\text{diss}}(X_2) = 5$ eV and 9 eV. c and f give $E_B^{\min}(X_2)$ as a function of the distance z to the surface i. e. the minimum of $E_B(X_2)$ relative to the intramolecular distance d for a given z . The corresponding values of d (in Å) are also given along these curves. $\Delta E^{\#}$ is the activation barrier for dissociation. The reference energy is the energy of two free X atoms.

Fig. 27 : Variation of the equilibrium energy of the molecule interacting with the substrate as a function of its dissociation energy (in units of E_{ads}) and geometry.

Fig. 28 : Equipotential energy curves (b) for an O_2 molecule approaching a (100) surface of a transition metal with a half filled d band (lattice parameter $a_0 = 3.16 \text{ \AA}$) according to the geometry of approach (a). The area limited by dotted lines shows the scanned region. The reference energy is the energy of two free O atoms.

Fig. 29 : Equipotential energy curves (b) for an O_2 molecule approaching a (110) surface of a transition metal with a half filled d band (lattice parameter $a_0 = 3.16 \text{ \AA}$) according to the geometry of approach (a). The area limited by dotted lines shows the scanned region. The reference energy is the energy of two free O atoms.

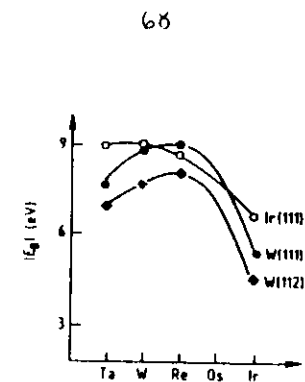


FIG. 1

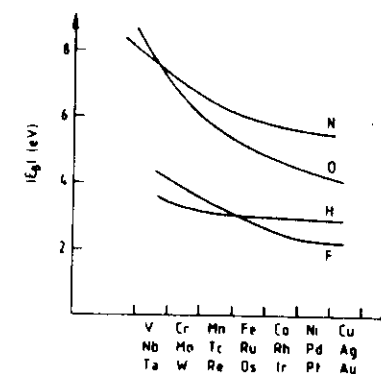


FIG. 2

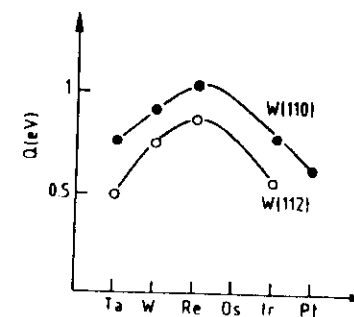


FIG. 3

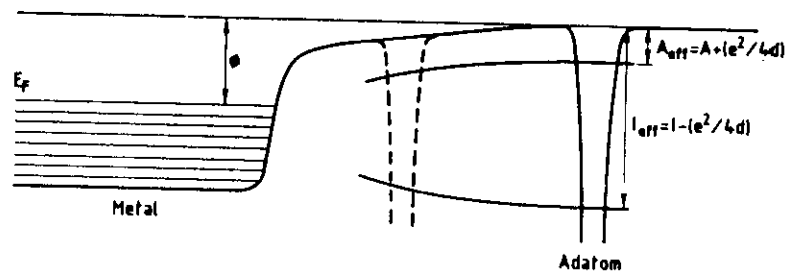


FIG. 4

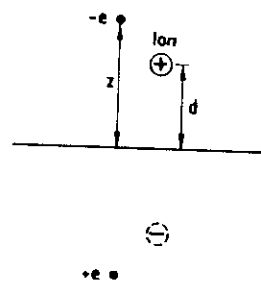
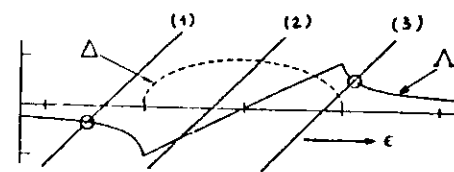
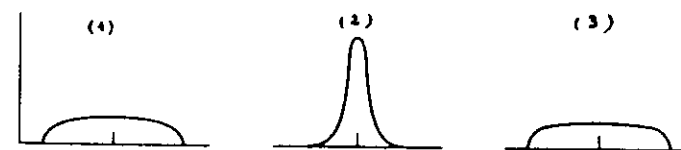


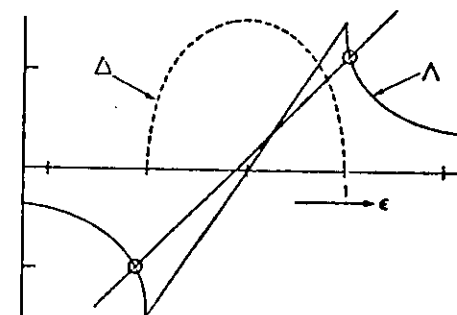
FIG. 5



(a)



(a')



(b)



(b')

FIG. 6

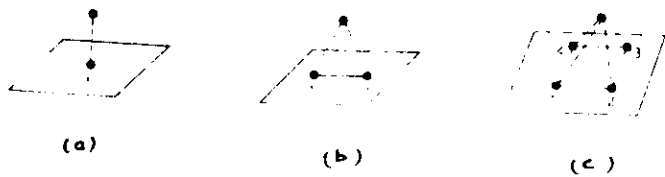


FIG. 7

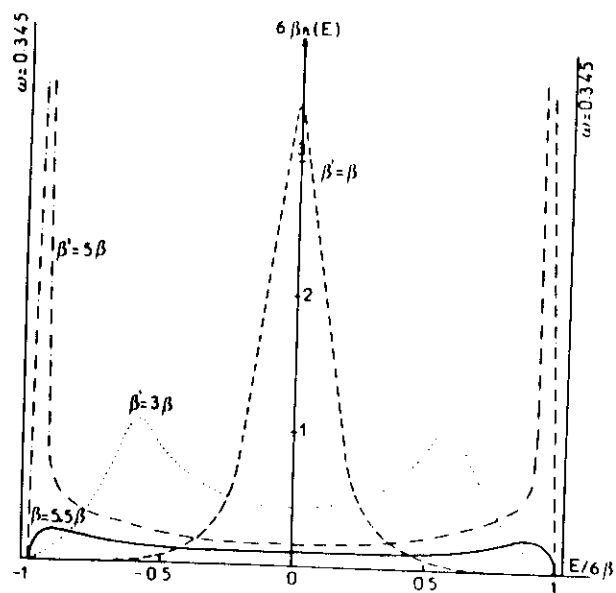


FIG. 8

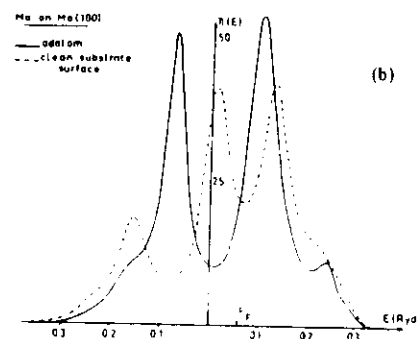
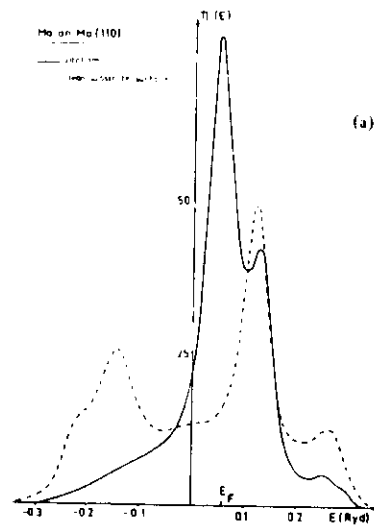
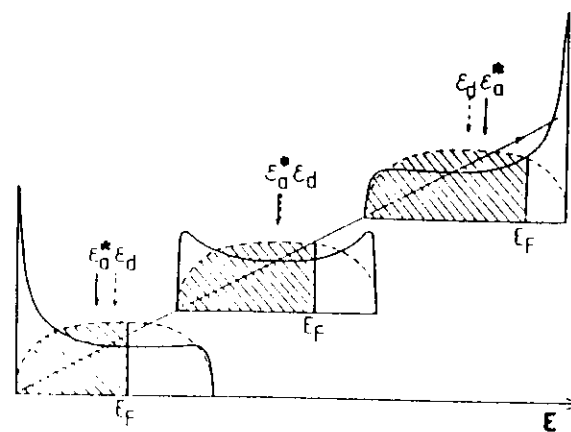


FIG. 9



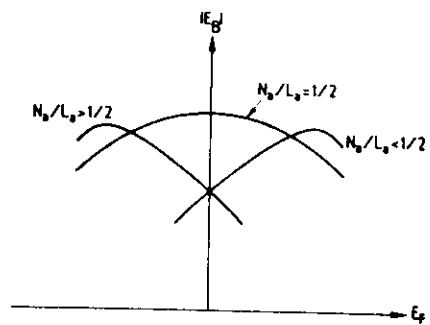


FIG. 11

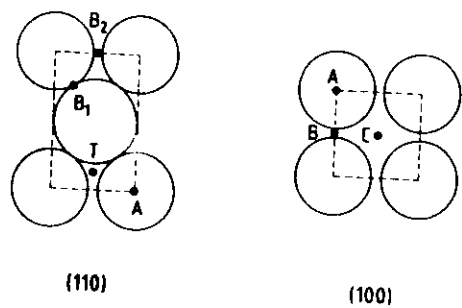


FIG. 12

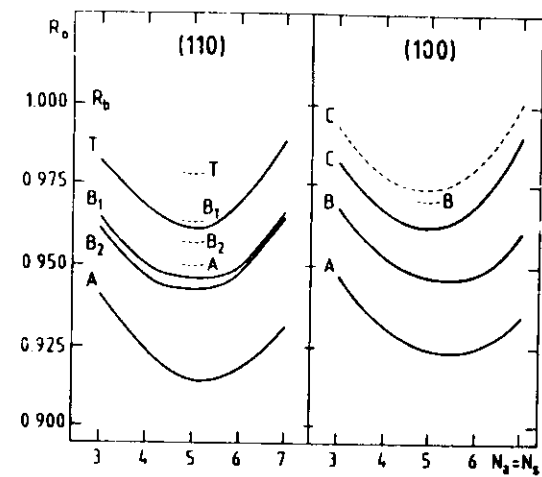


FIG. 13

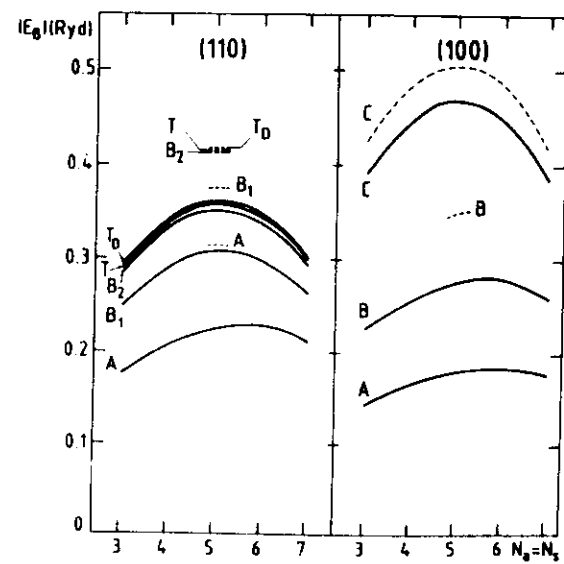


FIG. 14

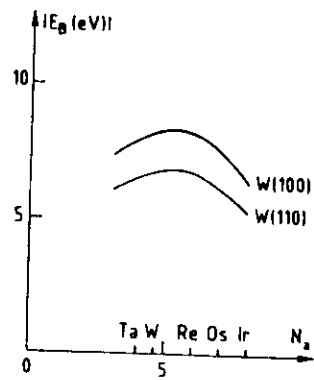


FIG. 15

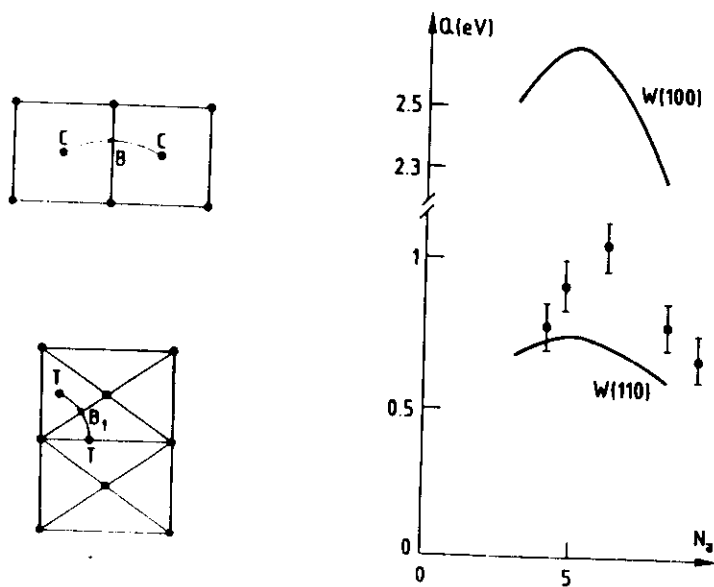


FIG. 16

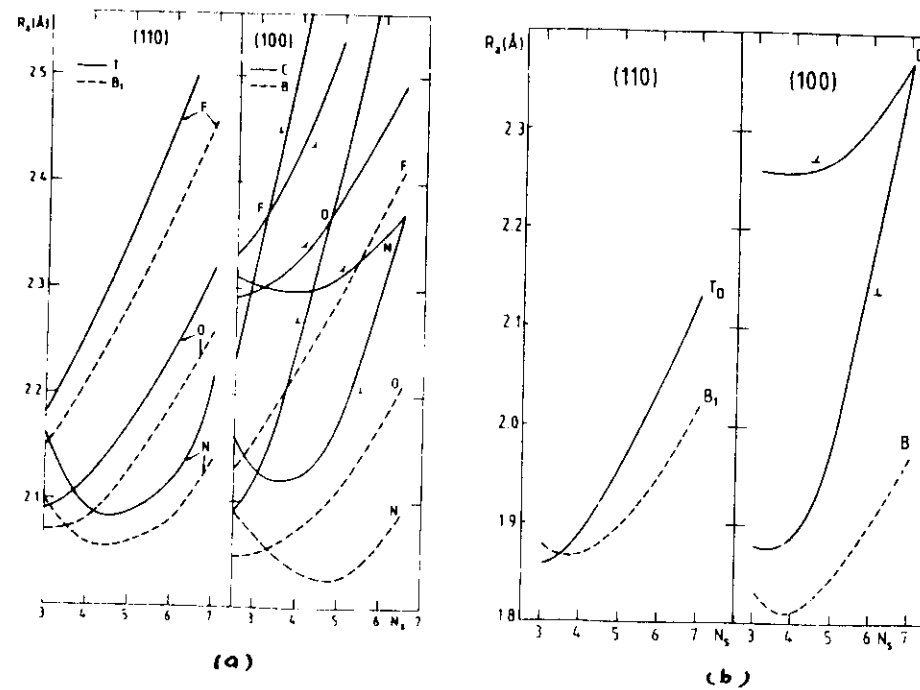


FIG. 17

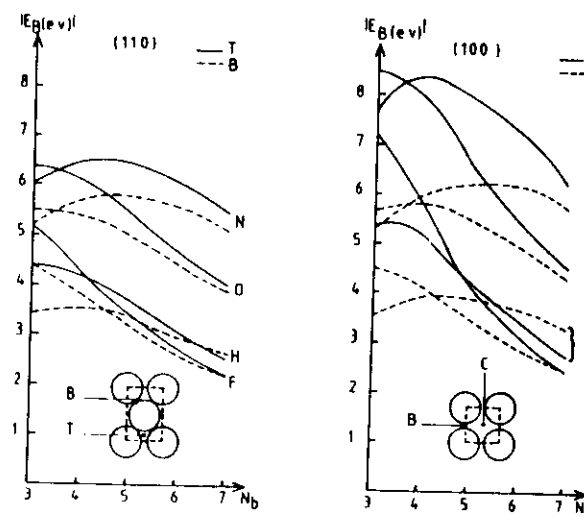


FIG. 18

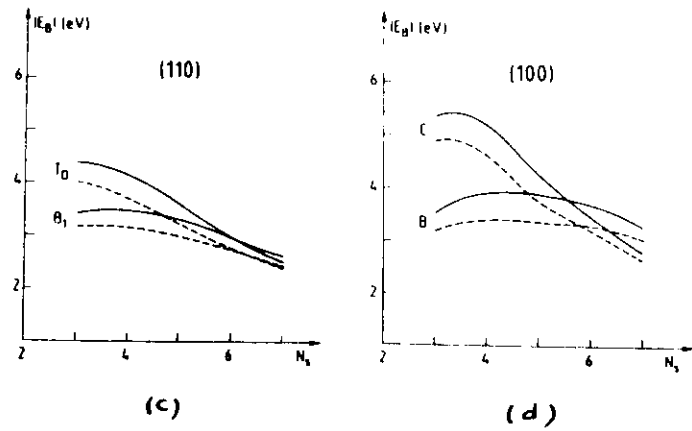
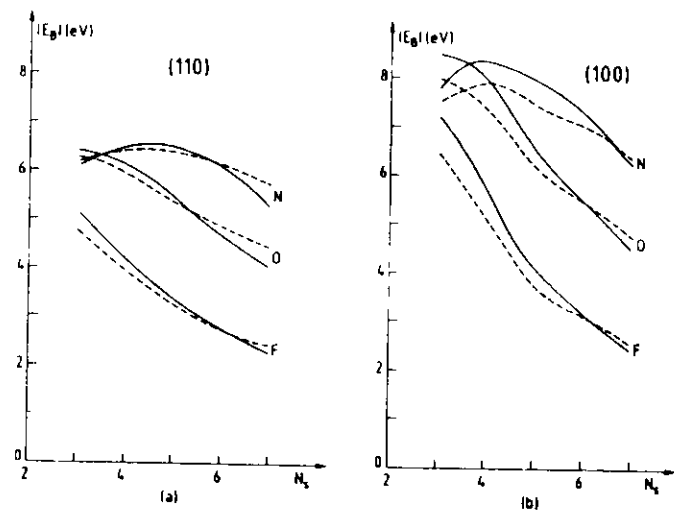
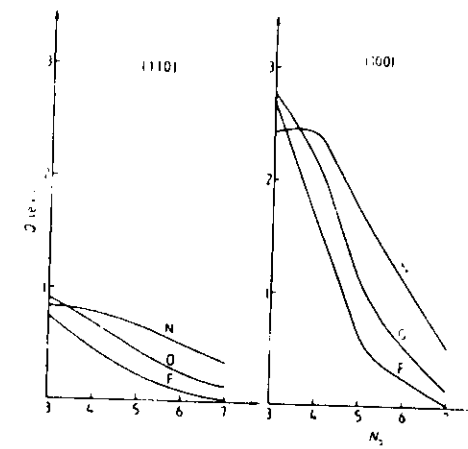
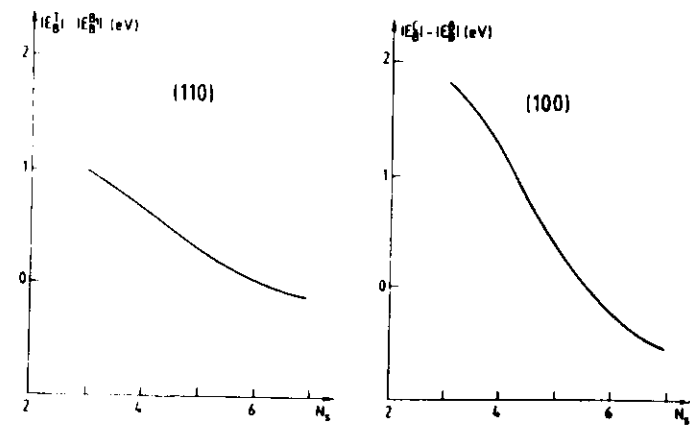


FIG. 19



(a)



(b)

FIG. 20

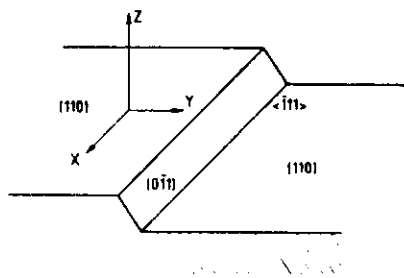


FIG. 21

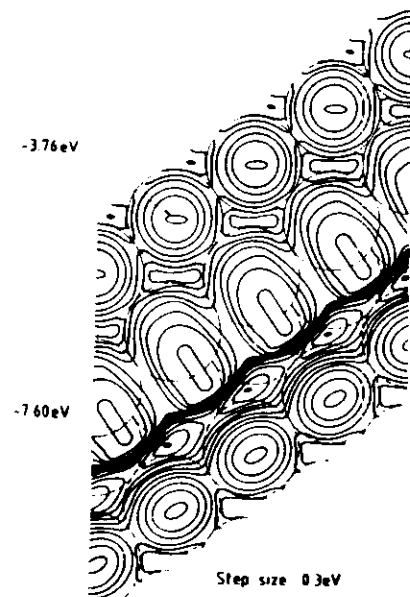
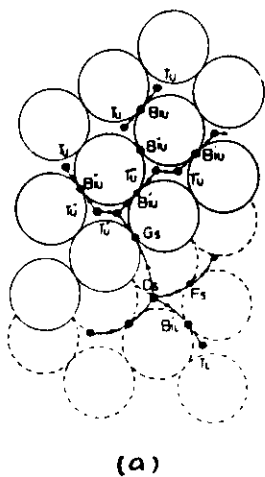
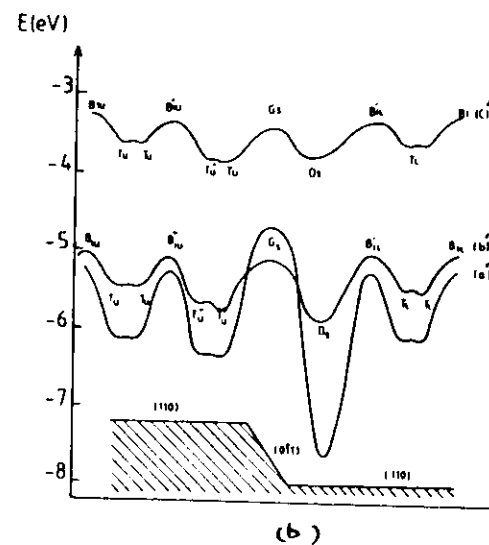


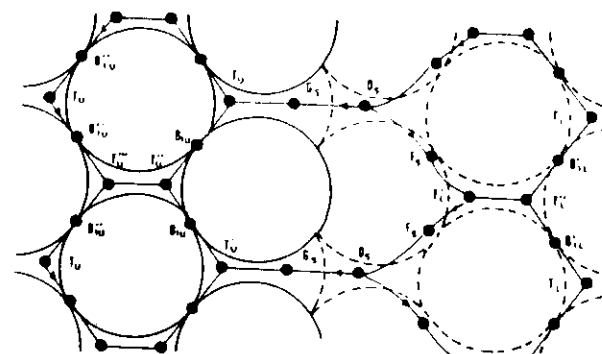
FIG. 22



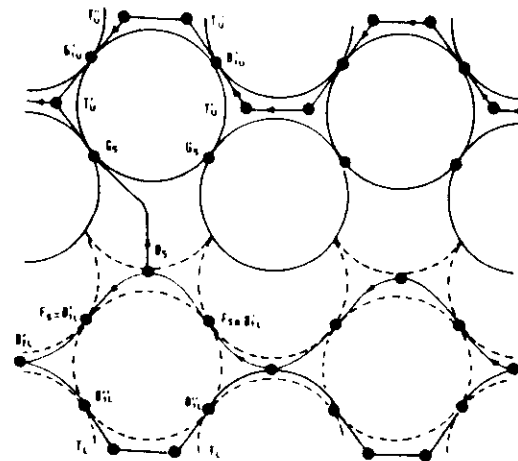
(a)



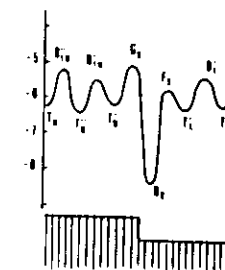
(b)



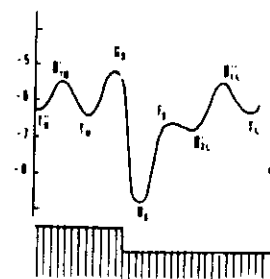
(a)



(b)



(a')



(b')

FIG. 24

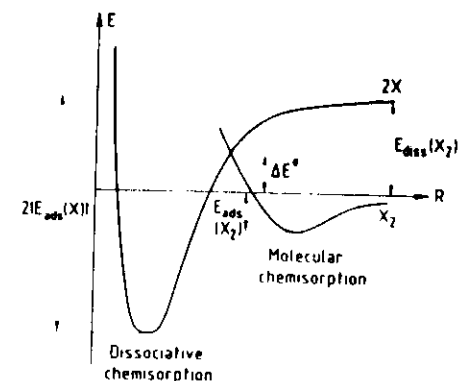
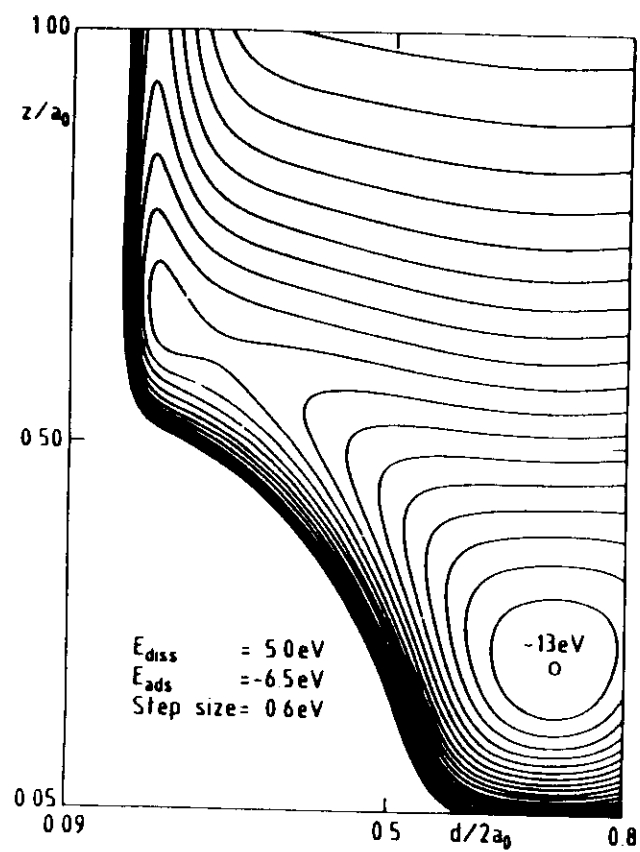
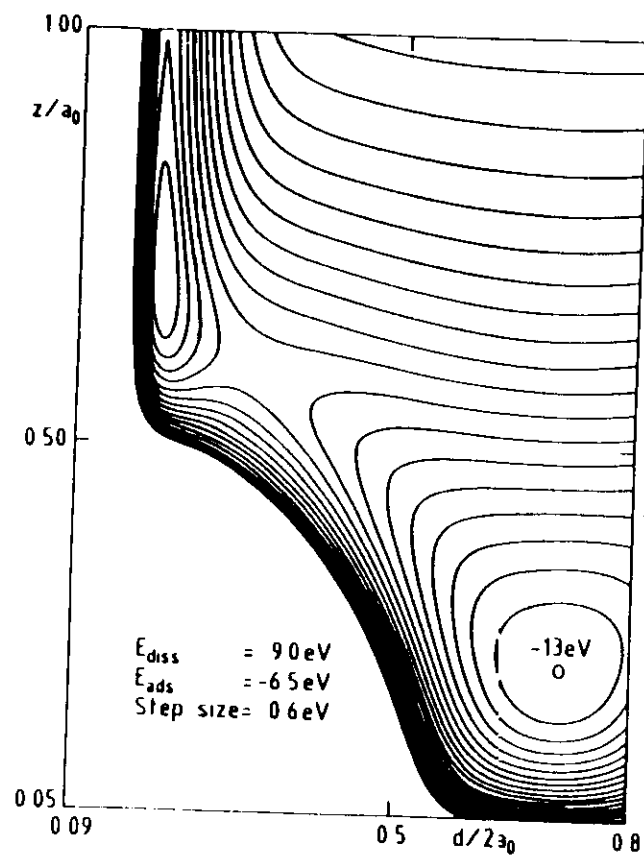


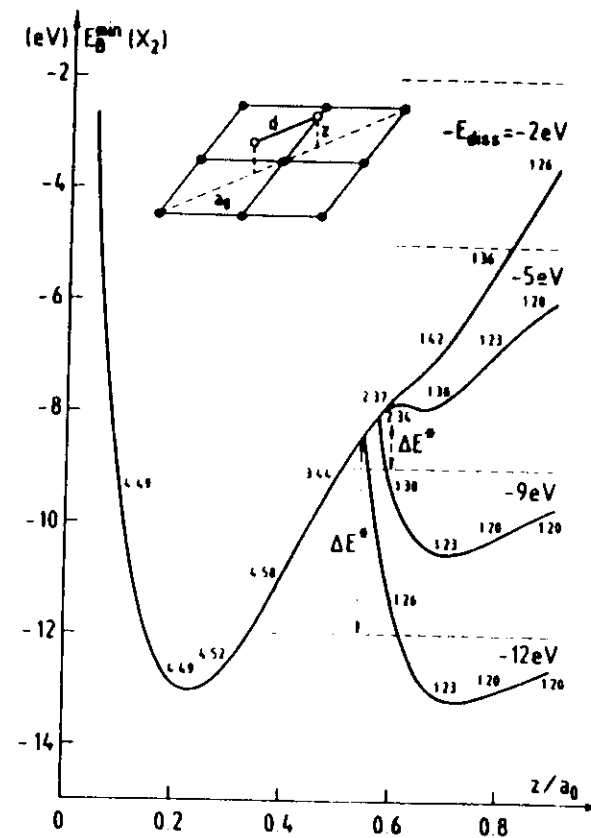
FIG. 25



(a)

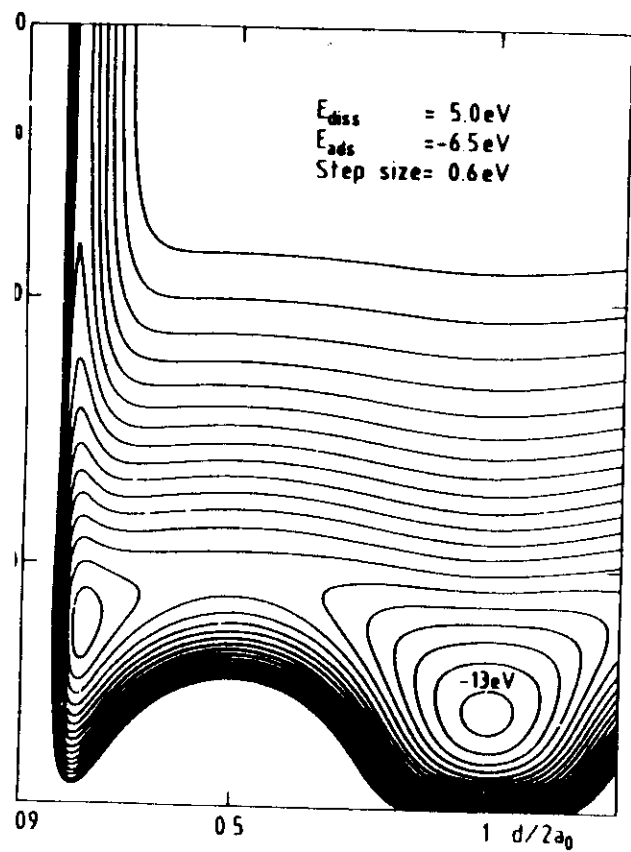


(b)

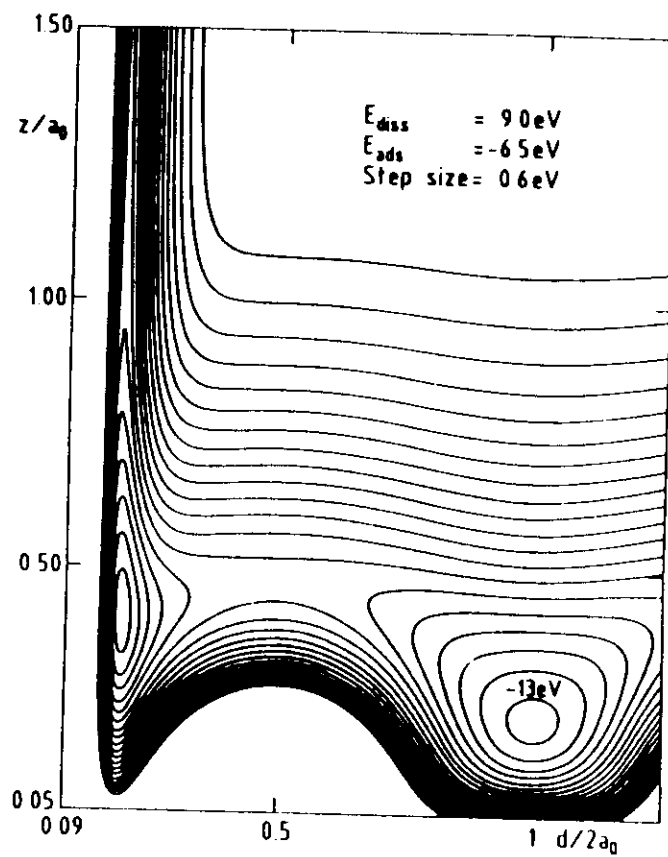


(c)

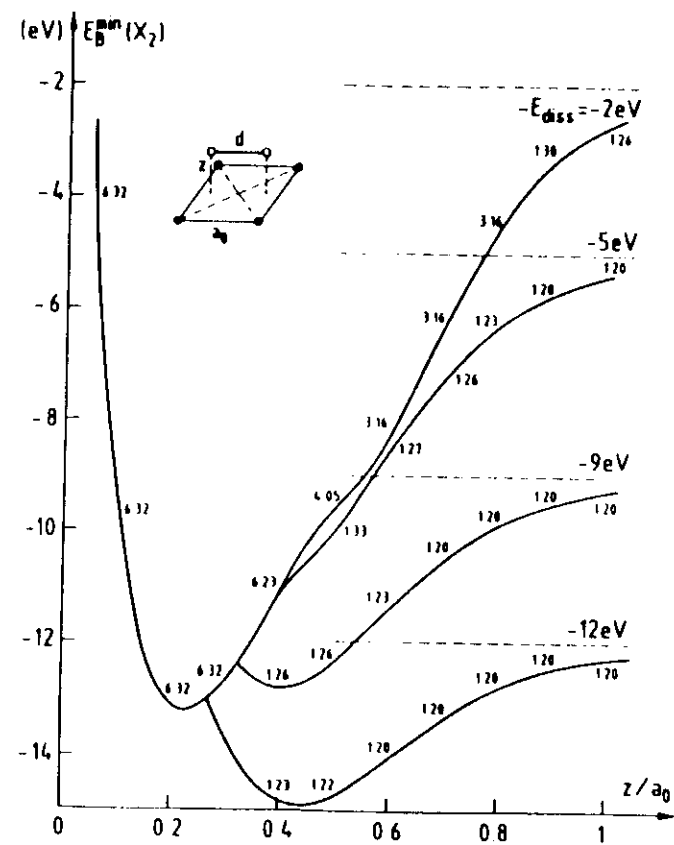
FIG. 26



(d)



(e)



(f)

FIG. 26

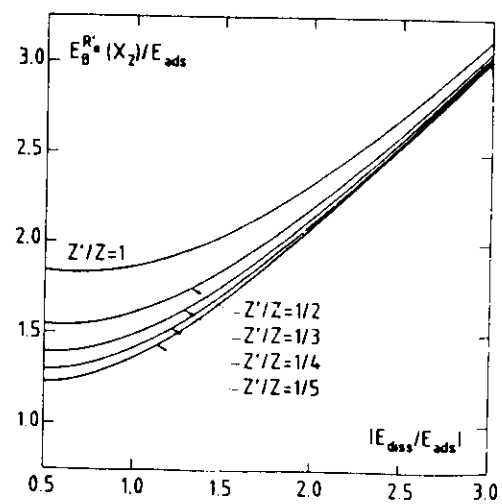


FIG. 27

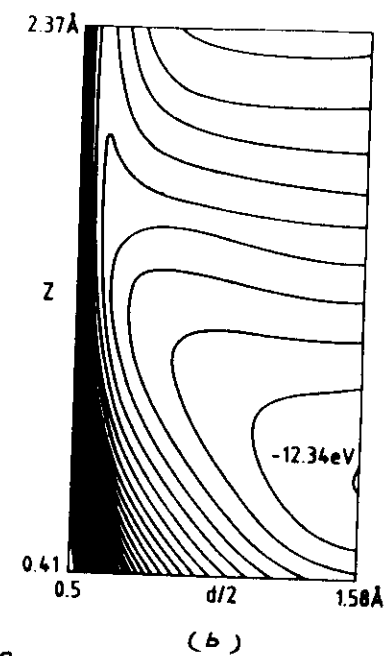
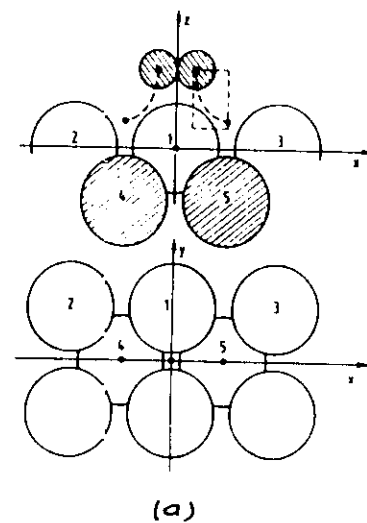


FIG. 28

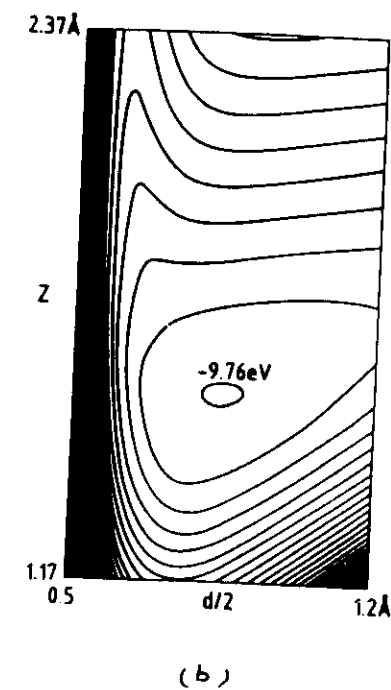
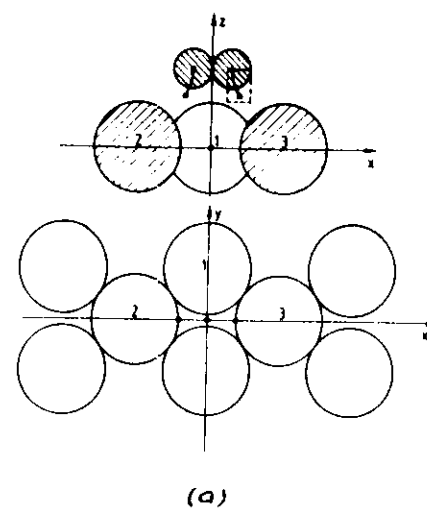


FIG. 29